ISSN 2523-6776

Volume 7, Issue 20 – July – December – 2023

# Journal of Technological Engineering

ECORFAN®

**Journal of Technological Engineering**, Volume 7, Issue 20, December 2023, is a journal published semi-annually by ECORFAN-Taiwan. Taiwan, Taipei. YongHe district, ZhongXin, Street 69. Postcode: 23445. WEB: www.ecorfan.org/taiwan, revista@ecorfan.org. Editor in Chief: SERRUDO-GONZALES, Javier. BsC. ISSN: 2523-6776. Responsible for the last update of this issue of the ECORFAN Informatics Unit. ESCAMILLA-BOUCHÁN Imelda, LUNA-SOTO, Vladimir, updated December 30, 2023.

# Journal of Technological Engineering

## Definition of Journal

## Scientific Objectives

Support the international scientific community in its written production Science, Technology and Innovation in the Field of Engineering and Technology, in Subdisciplines of sources innovation in electrical, engineering signal, amplification electrical, motor design science, materials in electrical power, plants management and distribution of electrical energies.

ECORFAN-Mexico, S.C. is a Scientific and Technological Company in contribution to the Human Resource training focused on the continuity in the critical analysis of International Research and is attached to CONACYT-RENIECYT number 1702902, its commitment is to disseminate research and contributions of the International Scientific Community, academic institutions, agencies and entities of the public and private sectors and contribute to the linking of researchers who carry out scientific activities, technological developments and training of specialized human resources with governments, companies and social organizations.

Encourage the interlocution of the International Scientific Community with other Study Centers in Mexico and abroad and promote a wide incorporation of academics, specialists and researchers to the publication in Science Structures of Autonomous Universities - State Public Universities - Federal IES - Polytechnic Universities - Technological Universities - Federal Technological Institutes - Normal Schools - Decentralized Technological Institutes - Intercultural Universities - S & T Councils - CONACYT Research Centers.

## Scope, Coverage and Audience

Journal of Technological Engineering is a Journal edited by ECORFAN-Mexico, S. C. in its Holding with repository in Taiwan, is a scientific publication arbitrated and indexed with semester periods. It supports a wide range of contents that are evaluated by academic peers by the Double-Blind method, around subjects related to the theory and practice of sources innovation in electrical, engineering signal, amplification electrical, motor design science, materials in electrical power, plants management and distribution of electrical energies with diverse approaches and perspectives, that contribute to the diffusion of the development of Science Technology and Innovation that allow the arguments related to the decision making and influence in the formulation of international policies in the Field of Engineering and Technology. The editorial horizon of ECORFAN-Mexico® extends beyond the academy and integrates other segments of research and analysis outside the scope, as long as they meet the requirements of rigorous argumentative and scientific, as well as addressing issues of general and current interest of the International Scientific Society.

## Editorial Board

## Arbitration Committee

**Assignment of Rights**

The sending of an Article to Journal of Technological Engineering emanates the commitment of the author not to submit it simultaneously to the consideration of other series publications for it must complement the Originality Format for its Article.

The authors sign the Authorization Format for their Article to be disseminated by means that ECORFAN-Mexico, S.C. In its Holding Taiwan considers pertinent for disclosure and diffusion of its Article its Rights of Work.

**Declaration of Authorship**

Indicate the Name of Author and Coauthors at most in the participation of the Article and indicate in extensive the Institutional Affiliation indicating the Department.

Identify the Name of Author and Coauthors at most with the CVU Scholarship Number-PNPC or SNI-CONACYT- Indicating the Researcher Level and their Google Scholar Profile to verify their Citation Level and H index.

Identify the Name of Author and Coauthors at most in the Science and Technology Profiles widely accepted by the International Scientific Community ORC ID - Researcher ID Thomson - arXiv Author ID - PubMed Author ID - Open ID respectively.

Indicate the contact for correspondence to the Author (Mail and Telephone) and indicate the Researcher who contributes as the first Author of the Article.

**Plagiarism Detection**

All Articles will be tested by plagiarism software PLAGSCAN if a plagiarism level is detected Positive will not be sent to arbitration and will be rescinded of the reception of the Article notifying the Authors responsible, claiming that academic plagiarism is criminalized in the Penal Code.

**Arbitration Process**

All Articles will be evaluated by academic peers by the Double Blind method, the Arbitration Approval is a requirement for the Editorial Board to make a final decision that will be final in all cases. MARVID® is a derivative brand of ECORFAN® specialized in providing the expert evaluators all of them with Doctorate degree and distinction of International Researchers in the respective Councils of Science and Technology the counterpart of CONACYT for the chapters of America-Europe-Asia- Africa and Oceania. The identification of the authorship should only appear on a first removable page, in order to ensure that the Arbitration process is anonymous and covers the following stages: Identification of the Journal with its author occupation rate - Identification of Authors and Coauthors - Detection of plagiarism PLAGSCAN - Review of Formats of Authorization and Originality-Allocation to the Editorial Board-Allocation of the pair of Expert Arbitrators-Notification of Arbitration -Declaration of observations to the Author-Verification of Article Modified for Editing-Publication.

**Instructions for Scientific, Technological and Innovation Publication**

**Knowledge Area**

The works must be unpublished and refer to topics of sources innovation in electrical, engineering signal, amplification electrical, motor design science, materials in electrical power, plants management and distribution of electrical energies and other topics related to Engineering and Technology.

## Presentation of Content

As first article we present, *Characterization of a dual system of hydraulic cylinders to originate tilting movement and column support in an industrial furnace*, by TÉLLEZ-MARTÍNEZ, Jorge Sergio, SÁNCHEZ-HERNÁNDEZ, Miriam Zulma, KANTUN-UICAB, María Cristina and PACHECO-SANTAMARÍA, Gerardo, with secondment at the Tecnológico Nacional de México / Instituto Tecnológico de Morelia, Universidad Politécnica de Juventino Rosas, as the second article we present, *Prediction model of a shell and tube heat exchanger based on the technique of artificial neural networks*, by TORRES-RICO, Luis, KOKU-TAMAKLOE, Elvis, MANRÍQUEZ-PADILLA, Carlos and VILLASEÑOR-AGUILAR, Marcos, with affiliation at the Universidad Politécnica de Juventino Rosas, Universidad Autónoma de Querétaro, Tecnológico Nacional de México - ITES de Irapuato, Universidad Politécnica de Guanajuato, as the third article we present, *Frutty-Pi (fruit sorter)*, by CORTES-GARCIA, Alicia, VALENCIA-GARCIA, Cesar Alejandro, SANTOS-OSORIO, Rene and RODRIGUEZ-MIRANDA, Gregorio, with affiliation at the Universidad Tecnológica de San Juan del Río, as last article we present, *Photovoltaic system design for electrical supply in a parkin lot*, by ESCOBEDO-MARQUEZ, Diana Laura, PALACIO-SIFUENTES, David Isaac, CASTILLO-CAMPOS, Nohemí Alejandra and ALVAREZ-MACIAS, Carlos, with assignment at the Tecnológico Nacional de México - Instituto Tecnológico de la Laguna.

## Content

Article **Journal of Technological Engineering**
December 2023, Vol.7 No.20 1-9

# Characterization of a dual system of hydraulic cylinders to originate tilting movement and column support in an industrial furnace

# Caracterización de un sistema dual de cilindros hidráulicos para originar movimiento basculante y del soporte en columna en un horno industrial

TÉLLEZ-MARTÍNEZ, Jorge Sergio´*†, SÁNCHEZ-HERNÁNDEZ, Miriam Zulma´, KANTUN-UICAB, María Cristina´´ and PACHECO-SANTAMARÍA, Gerardo´´´

´*Tecnológico Nacional de México / Instituto Tecnológico de Morelia, Morelia 58120, México.*
´´*Universidad Politécnica de Juventino Rosas. Procesos de Manufactura y Materiales Avanzados. Miguel Hidalgo 102, Comunidad de Valencia, Santa Cruz de Juventino Rosas, Gto.; México.*
´´´*Universidad Politécnica de Juventino Rosas. Academia de Ingeniería en Manufactura Avanzada. Miguel Hidalgo 102, Comunidad de Valencia, Santa Cruz de Juventino Rosas, Gto.; México.*

ID 1st Author: *Jorge Sergio, Téllez-Martínez* / **ORC ID:** 0000-0003-0587-0059, **CVU CONAHCYT ID:** 40084

ID 1st Co-author: *Miriam Zulma, Sánchez-Hernández* / **ORC ID:** 0000-0001-6230-6986

ID 2nd Co-author: *María Cristina, Kantun-Uicab* / **ORC ID:** 0000-0003-1588-5414, **CVU CONAHCYT ID:** 162342

ID 3rd Co-author: *Gerardo, Pacheco-Santamaría* / **ORC ID:** 0009-0004-2105-5171, **CVU CONHACYT ID:** 348373

**DOI**: 10.35429/JTEN.2023.20.7.1.9 Received July 10, 2023; Accepted December 30, 2023

**Abstract**

The controlled displacement of large masses or response to loads is guaranteed by implementing hydraulic systems. The capacity of these systems implies the cylinders' design and the pump power that drives the working fluids. In this regard, the reference to the construction planning of an industrial melting furnace is an example of analysis. Before determining the characteristics of the implicit hydraulic systems, the required element displacement magnitudes were determined. In addition to the load profiles according to the geometric and density characteristics of the materials used to consolidate the equipment during operating conditions, the data obtained by applying reaction analysis and the concept of force multiplication (Pascal's law) determined the equipment characteristics. Likewise, these characteristics are used to select the commercial elements, considering a safety factor for good performance.

**Angle joint design, Hydraulic systems, Assisted displacement**

**Resumen**

El desplazamiento controlado de grandes masas o respuesta a cargas se garantiza con la implementación de sistemas hidráulicos. La capacidad de estos sistemas implica el diseño de los cilindros y de la potencia de la bomba que impulse el fluido de trabajo. Al respecto, la referencia a la planeación de construcción de un horno de fusión industrial se utiliza como un ejemplo de análisis. Previo a la determinación de las características de los sistemas hidráulicos implícitos se determinaron las magnitudes de desplazamiento de elementos requeridas. Además de los perfiles de carga de acuerdo con las características geométricas y de densidad de los materiales utilizados en la consolidación del equipo durante condiciones operativas. Los datos obtenidos aplicando el análisis de reacciones y el concepto de multiplicación de fuerza (Ley de Pascal) se determinaron las características del equipo. Asimismo, estas características se utilizaron para la selección de elementos comerciales considerando un factor de seguridad para un buen desempeño.

**Diseño de articulaciones angulares, Sistemas hidráulicos, Desplazamiento asistido**

**Citation:** TÉLLEZ-MARTÍNEZ, Jorge Sergio, SÁNCHEZ-HERNÁNDEZ, Miriam Zulma, KANTUN-UICAB, María Cristina and PACHECO-SANTAMARÍA, Gerardo. Characterization of a dual system of hydraulic cylinders to originate tilting movement and column support in an industrial furnace. Journal of Technological Engineering. 2023. 7-20:1-9.

* Correspondence from the Author (E-mail: jorge.tm@morelia.tecnm.mx)
† Researcher contributing as first author.

 

## Introduction

In the hydraulic loading power systems terminology, piston cylinders are also called skid steer loaders used in various devices. For example, researchers (Dadhania, Bhatiya, Joshi, & Sharma, 2016) conducted a literature review on the design of the tilting mechanism of cabins in loading vehicle. These work vehicles also implement complex displacement systems controlled by hydraulic cylinders. Researchers (Xu & Yoon, 2016) reviewed the kinematic and dynamic modeling of the mechanical link in assisted blade joints and presented several modeling approaches in the hydraulic system. Other analyses of multiple cylinders acting on platforms are sparsely reported (Hu, et al., 2022), (Sun & Chiu, 2001). In the case of commercialized tilting furnaces, it is evident that the design of hydraulic systems is standardized and developed by the companies that manufacture them, (Nabertherm, 2023). However, design engineering information is confidential except in the corresponding patents or some incipient reports at conferences (Audet, Parent, Deveaux, & Courtenay, 2004).

**Figure 1** Melting furnace implementing: a) joint for tilting, b) joint for opening the lid
*Source: Images property of Mechatronics DDMI COMBUSTION.*
*https://www.youtube.com/watch?v=LP3Wmo8rSlU*

Therefore, through the analysis of the trajectory of joint displacements and a force balance based on reactions, it was proposed to obtain the characteristics of hydraulic cylinders with specific loading conditions for the construction of equipment similar to that shown in Figure 1, and to define the programming bases of a computer application that allows calculating variants. The objective was to obtain an analysis methodology for characterizing hydraulic cylinders acting in pairs in a symmetrical system considering a pseudo-static load. Given the extent of development of this work, a work published simultaneously by the primary author supports the analysis of the geometry of assisted joints implemented for tilting.

## Methodology

Reaction analysis consists of making equilibrium diagrams of the system subjected to loads. Addressing the two cases relevant to determining the analysis strategy allows us to understand the objective results. First, the standard operating position of the furnace suggests that the joint system is in a static state, forming a frame of two vertical columns and a beam, as shown in **Figure 2**. In this case, the model scheme presents two fixed support points, A and B, determining a system for hyperstatic analysis. However, due to the hinge at point C, the system can be decomposed into two separate subsystems that simplify the formulation.

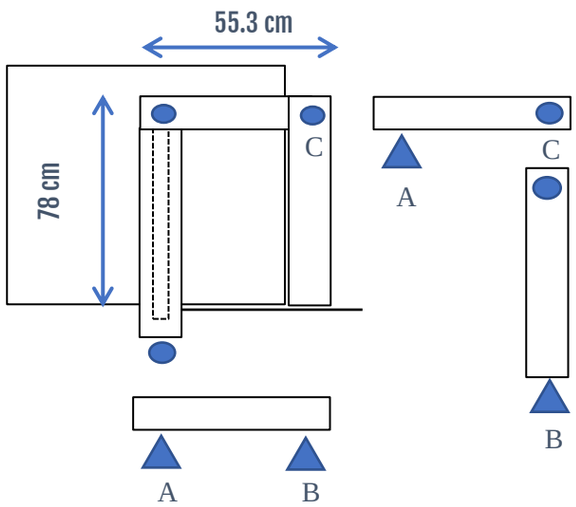


**Figure 2** Scheme of the system in a static state for the analysis of reactions proposed with a hyper-static gantry system and as two separate systems due to the existence of the kneecap at point C
*Source: Own creation in Microsoft PowerPoint 2016.*

ISSN 2523-6776

The system with fixed support at point A must be formulated in the rest condition and during the tilting trajectory. In this way, the schematization of the balance diagrams for both conditions corresponds to the information shown in **Figures 3(a) and 3(b)**, respectively (Nelson, Best, McLean, & Potter, 2010).

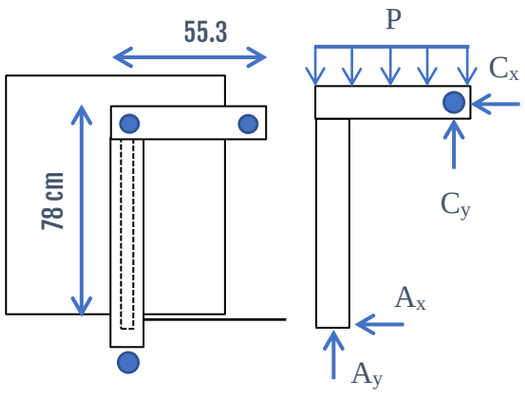


**(a)**

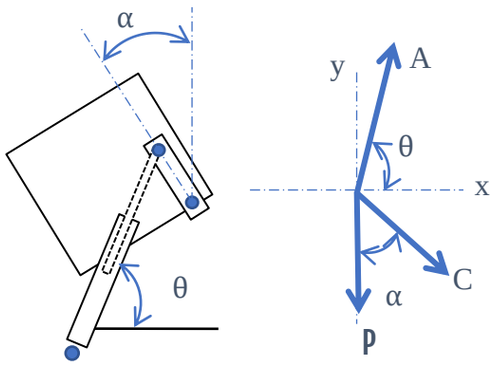


**(b)**

**Figure 3** Diagrams of the system with fixed support at point A under conditions of: a) rest and b) in trajectory during tilting
*Source: Own creation in Microsoft PowerPoint 2016.*

In the case of the rest position, the balance at point A responds to the reactions $A_x$ and $A_y$ with an effect on C due to the distributed load P. **Equation 1** determines the moment balance about point A.

$$\sum M_A = 0 \rightarrow = \sum M_{A\circlearrowright} + \sum M_{A\circlearrowleft} \quad (1)$$

In this way, **Equation 2** results from the analysis of the clockwise and counterclockwise moments of **Figure 3(a)**.

$$\frac{PL}{2} = \frac{PL}{2} + C_x H + C_y L \rightarrow C_y = -C_x \frac{H}{L} \quad (2)$$

In the balance of forces, **Equations 3 and 4** determine the relationship between the components corresponding to points A and C concerning the influence of P.

$$\sum F_{x,A} = 0 \rightarrow A_x = -C_x \quad (3)$$

$$\sum F_{y,A} = 0 \rightarrow A_y + C_y = P \quad (4)$$

Due to the distributed load of P over the section of length L, the system has load symmetry about points A and C. Such that:

$$A_y = C_y = \frac{1}{2}P \quad (5)$$

In this way, calculating the magnitudes of $A_x$ and $C_x$ depends on **Equations 2 and 3**.

$$C_x = -\frac{PL}{2H}; \quad A_x = \frac{PL}{2H} \quad (6)$$

On the other hand, in a trajectory position during tilting, the directions of the resulting forces A and C depend, respectively, on the angles α and θ. Under conditions of instantaneous equilibrium, **Equations 7 and 8** determine the force balance for the scheme in **Figure 3(b)**.

$$\sum F_x = 0 = A\cos(\theta) + C\,sen(\alpha) \quad (7)$$

$$\sum F_y = 0 = A\,sen(\theta) - C\cos(\alpha) - P \quad (8)$$

To know the charge P with the solution of a system of two equations with two unknowns, C is solved for **Equation 7**, defining **Equation 9**.

$$C = -A\frac{\cos(\theta)}{sen(\alpha)} \quad (9)$$

**Equation 10** arises by substituting **Equation 9** in **Equation 7** and solving for A, which determines the load experienced at this point, equivalent to the load or force that the cylinder piston overcomes during expansion, that is, in clamping with the furnace.

$$A = \frac{P\,sen(\alpha)}{sen(\theta)sen(\alpha) + \cos(\theta)\cos(\alpha)} \quad (10)$$

ISSN 2523-6776

Calculating the load conditions in each furnace position during tilting depends on **Equations 9, 8, and 3**. Therefore, in the balance of moments about point B, defined by **Equation 11**, the magnitude of the moment is to be counteracted due to the tilting effect.

$$\sum M_B = 0 \rightarrow = \sum M_B\circlearrowright + \sum M_B\circlearrowleft \quad (11)$$

The scheme in **Figure 4** and **Equation 11** establishes that the charges $C_y$, $B_y$ and $C_x$ are absorbed by the attachment point B and gives rise to **Equation 12**.

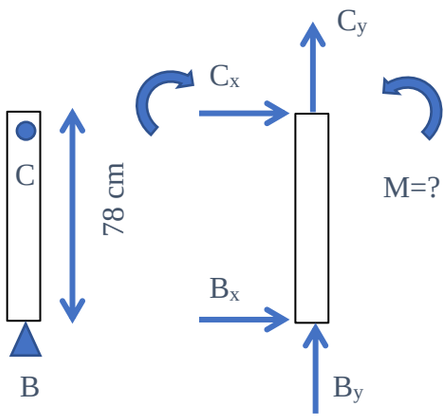


**Figure 4** Scheme of reactions in the fixed column with support at point B
*Source: Own creation in Microsoft PowerPoint 2016.*

$$C_x H = M \quad (12)$$

If a force w existed, keeping the column balanced with the reactions $C_x$ and $B_x$, **Equation 12**, rewritten as **Equation 13**, indicates that there is a direct proportionality.

$$C_x H = wH\left(\frac{H}{2}\right) \rightarrow C_x = w\left(\frac{H}{2}\right) \quad (13)$$

Obtaining each system component involved in the force balance in the analysis directions depends on **Equations 14 and 15**.

$$\sum F_x = 0 = C_x + B_x \rightarrow C_x = -B_x \quad (14)$$

$$\sum F_y = 0 \rightarrow B_y = C_y \quad (15)$$

On the other hand, the maximum applicable load w depends on the analysis of the profile's resistance capacity used for the column's construction. **Figure 5** shows the internal load diagrams for the conditions of shear force V and bending moment $M_f$, corresponding to the proposed uniformly distributed load w. The maximum bending moment develops in the shear force plane located at H/2 and is defined by **Equation 16**.

$$M_{fmax} = \frac{1}{4}wH^2 = C_x\frac{H}{2} \quad (16)$$

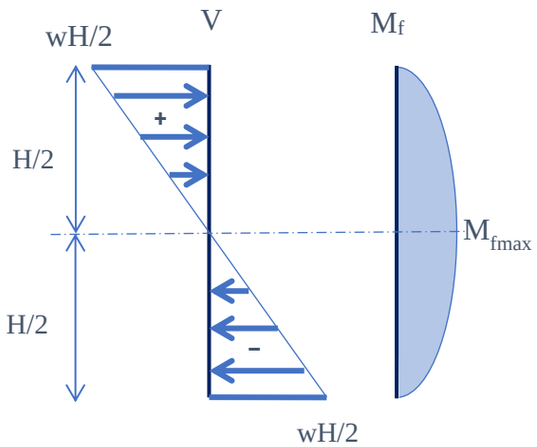


**Figure 5** Shear force and bending moment diagrams
*Source: Own creation in Microsoft PowerPoint 2016.*

While **Equation 17** as defines shear stress:

$$\tau = \frac{VQ}{Ib} \quad (17)$$

Where $b$ is the critical thickness of the profile corresponding to the neutral axis, $I$ represents the moment of inertia, $Q$ is the first-order moment, and $V$ is the maximum shear force, as, for example, for an IPS or IS beam, which has an H-shaped cross-section as shown in **Figure 6**.

ISSN 2523-6776

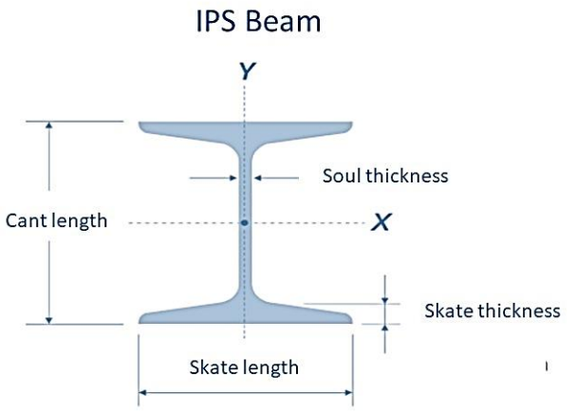


**Figure 6** Cross-section drawing of IPS Beam
*Source: Image property of (MIPSA, 2023).*

**Equation 18** allows determining the moment of inertia considering the geometry of the cross-section of the column and the plane on the X-axis (centroid). The corresponding calculation quantifies the cross-sectional surface of the solid shown in **Figure 6**, creating bounded sub-regions in rectangles; the data bf and h represent the length magnitudes of the base and height sides, respectively.

$$I = \frac{b_f h^3}{12} \tag{18}$$

In a similar way, the first-order moment $Q$ is estimated by calculating the sum of the areas of each sub-region bounded by rectangles multiplied by the distance of the centroid of each rectangle to the position of the median plane, considering only the geometric region above the plane concerning the centroid or upper module in the beam.

According to the equilibrium system proposed in **Figure 4**, the magnitude of the shear force V determined through the reaction analysis of the system in **Figure 3(b)** would already be known. Therefore, according to the magnitude of the maximum shear force developed at the support points C and B in **Equation 17**, the maximum shear stress that the material must possess to avoid failure is obtained.

Finally, **Equation 19** defines the stress in the spine due to the bending moment, where c represents the distance from the centroid of the beam to the farthest fiber.

$$\sigma = \frac{Mc}{I} \tag{19}$$

In the case of **Figure 6**, $c$ corresponds to the distance between the position of the X plane and the edge of the beam cant. Therefore, the maximum stress determining the most significant flexion in the spine depends on the ultimate flexor moment.

## Results

**Equations 20, 21, and 22** determine the displacement trajectories in the articulated element for tilting the furnace schematized in **Figure 7**. Determining the angles α and θ supports the analysis of reactions and determination of forces according to **Figure 3(b)**. **Graphic 1** shows the curves corresponding to these angles as a function of the length of displacement directed by the piston of the hydraulic cylinders.

$$\boldsymbol{a}^2 = \boldsymbol{x}^2 + \boldsymbol{y}^2 \tag{20}$$

$$L^2 = (\boldsymbol{y} - H)^2 + (L - \boldsymbol{x})^2 \tag{21}$$

$$\begin{aligned} \boldsymbol{y}^2(4L^2 + 4H^2) - \boldsymbol{y}(4H^3 + 4\boldsymbol{a}^2 H) \\ + (2\boldsymbol{a}^2 H^2 - 4\boldsymbol{a}^2 L^2 + H^4 \\ + \boldsymbol{a}^4) = 0 \end{aligned} \tag{22}$$

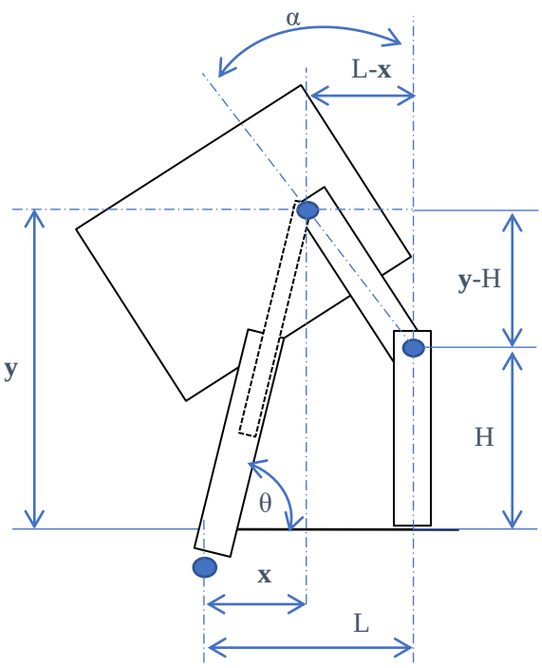


**Figure 7** Geometric analysis of the joints for furnace tilting
*Source: Own creation in Microsoft PowerPoint 2016*

ISSN 2523-6776

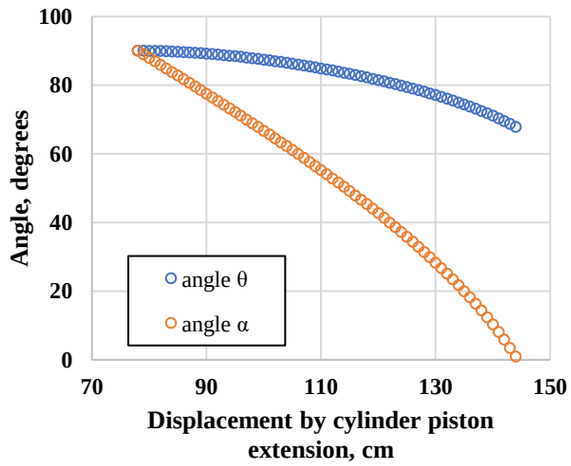


**Graphic 1** Curves of the evolution of the angles α and θ defined in the scheme of **Figure 7**
*Source: Own creation in Microsoft Excel 2016.*

Firstly, determine the magnitude of the force experienced at point A, equivalent to obtaining C according to **Equation 3**. Graphic 2 shows the variation depending on the extension of the cylinder piston and, consequently, the amount of rotation during tilting.

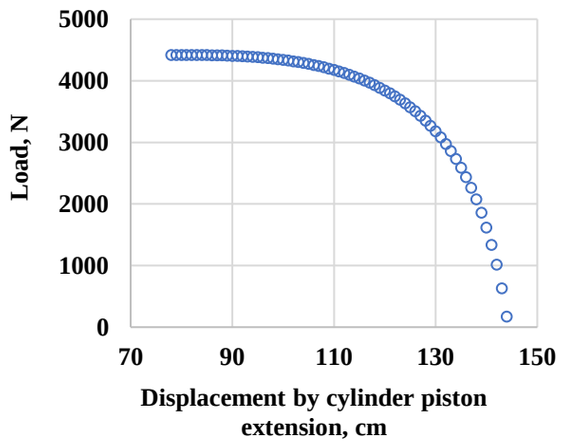


**Graphic 2** Curves of the magnitude of the force experienced at point A according to the scheme in **Figure 3(b)**
*Source: Own creation in Microsoft Excel 2016.*

Interestingly, the force at point A decreases to almost zero once the furnace has reached the fully tilted position logically because the load at that point is a reaction on point B transferred by the column or post. The magnitude of the force experienced at point C corresponds to the sum of the shear and axial forces acting on the column supported at point B, as shown by the curves in **Graphic 3**.

While the axial force is always incremental, the cutting force acquires a maximum ($V_{max}$) before the full tilt position (α = 25º and θ = 76º) and subsequently decreases to an almost zero condition.

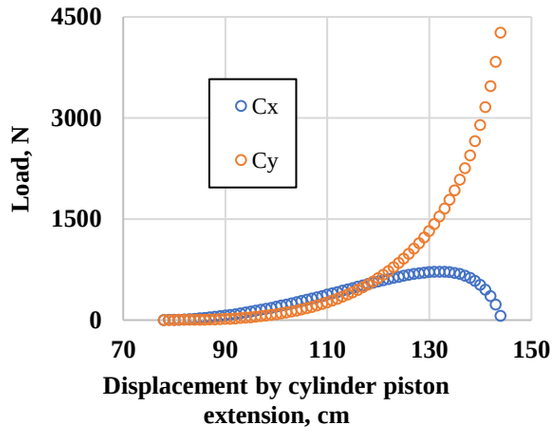


**Graphic 3** Curves of the magnitude of the force of the components of the resultant at point C according to the scheme of Fig. 3(b)
*Source: Own creation in Microsoft Excel 2016*

The magnitudes represented by the curves in **Graphs 2 and 3** correspond to the assumed calculation of a furnace mass in operation of 900 kg. Therefore, according to the load distribution, each system directed on the flanks of the furnace equally supports 4414.5 N. According to this information, **Equations 18 and 19** allow us to obtain the shear stress at point C during the tilting of the furnace and the stress generated in the plane of the maximum bending moment, which is located halfway up the column. (See the curves in **Graph 4**). The calculation of the moment of inertia *I* determined a magnitude of 5070054.48 $mm^4$, while the first order moment *Q*, with a magnitude of 45795.46 $mm^3$, considering the following IPS profile specification:

- Cant Length: 127 mm
- Skate Length: 76.3 mm
- Core Thickness: 5.44 mm
- Skate Thickness (average): 8.28 mm
- Location of the centroid plane X: 63.5 mm

ISSN 2523-6776

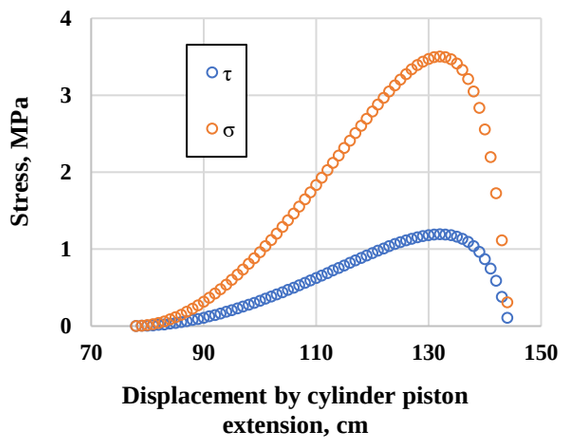


**Graphic 4** Curves of the magnitude of shear stress experienced at point C and the stress at mid-height of the column in the plane of development of the bending moment Mf, according to the scheme in **Figure 5**
*Source: Own creation in Microsoft Excel 2016.*

Regarding the magnitudes of stress, the maximums of both shear and bending coincide with α = 25º and θ = 76º, only considering the shear force $C_x$. However, there is the axial load associated with the $C_y$ component. The Von Mises criterion provides an equation for determining the static strength criterion and, therefore, the contribution of the compressive load experienced by the column to the maximum shear stress.

In this regard, the calculation of w using **Equation 13** corresponds to the distributed load acting on the column in the direction perpendicular to the compression direction. Such that:

$$w = \frac{2}{H} C_x \tag{23}$$

By definition, the biaxial stress state relates the force $C_y$ through **Equation 24** to the shear stress by principal stresses (Dieter, 1986).

$$\tau_{comp} = \frac{1}{2}\left(\frac{C_y}{S_1} - \frac{w}{S_2}\right) \tag{24}$$

$S_1$ and $S_2$ represent the surfaces of the beam where the forces of the main directions act (1: axial, 2: transverse). In this way, the magnitude of $w$ determines the influence of the perpendicular direction (2) on the compression direction (1). However, in this case, it does not modify the generation of shear stress $\tau_{\_comp}$ due to the magnitude of the surface $S_2$.

**Graph 5** presents the curves corresponding to the magnitude of the principal stresses experienced in the column in each furnace position during tilting.

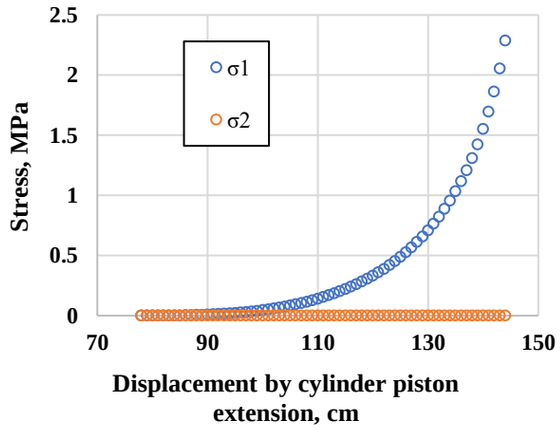


**Graphic 5** Curves of the magnitude of principal stresses experienced in the column during the tilting of the furnace
*Source: Own creation in Microsoft Excel 2016.*

**Graphic 6** compares the magnitude of the shear stress in the beam calculated from **Equation 24** with that calculated through **Equation 7**. Note that each case's maximum magnitude of the shear stress is similar. However, in a different tilting condition of the furnace, since, in the case of effect due to principal stresses, the maximum shear stress $\tau_{comp}$ is found in the position α = 0.84º and θ = 67.76º or at the end of the total rotation about point C. However, when considering the addition of the shear stresses for the point of maximum influence defined by **Figure 5**, there is a critical interval for α between 25° and 0.84° and for θ between 76° and 67.76°, with the maximum at α = 16.26º and θ = 73.1°.

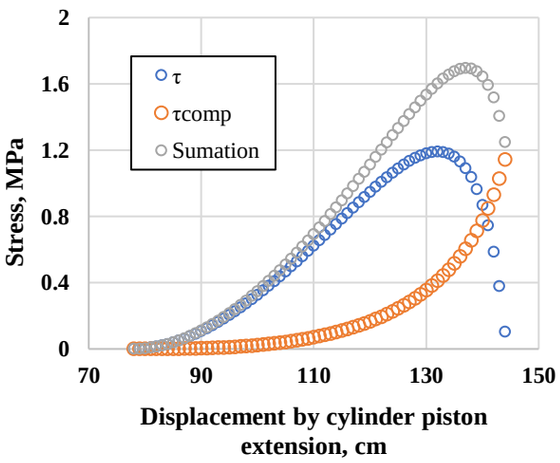


**Graphic 6** Curves of the magnitude of shear stresses experienced in the column during the tilting of the furnace
*Source: Own creation in Microsoft Excel 2016*

Defining the Von Mises criterion through **Equation 25** (maximum distortion energy criterion), the magnitude of the estimated stress value due to the effect of the principal stresses determines that the material will not flow if the stress is less than the recorded as the yield of the manufacturing material of the beam that makes up the column; and that in the adopted case corresponds to the IPS structure.

$$\sqrt{\frac{1}{2}((\sigma_1-\sigma_2)^2+(\sigma_1-\sigma_3)^2+(\sigma_2-\sigma_3)^2)} < \sigma_y \quad \textbf{(25)}$$

Since a principal stress acting from a third direction acting from a third direction is not considered, Eq. 25 reduces to the expression of Eq. 26.

$$\sqrt{\frac{1}{2}((\sigma_1-\sigma_2)^2+{\sigma_1}^2+{\sigma_2}^2)} < \sigma_y \quad (26)$$

**Graphic 7** shows the result of calculating the effort of the Von Mises criterion. In the curve (empty blue circles), the same behavior shown by the shear stress ($\tau_{comp}$) is identified, although the magnitude is double the amount. Therefore, the maximum state of stress in the column coincides with the position of the furnace in total elevation or at the end of the tilt. Again, the critical interval corresponds for α between 25° and 0.84° and θ between 76° and 67.76°, with the maximum now at α = 18.12º and θ = 73.73° in this case in the position of occurrence of the bending moment.

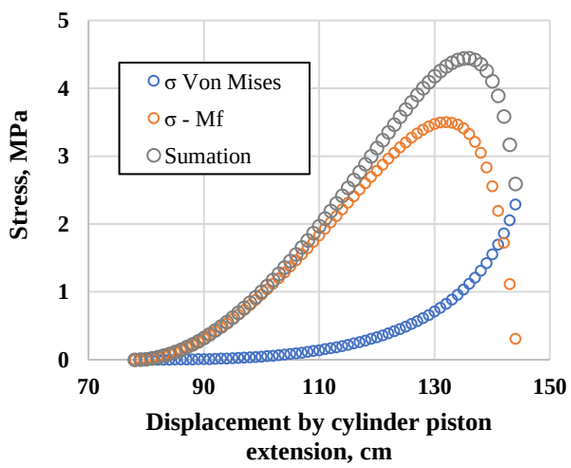


**Graphic 7** The magnitude of the Von Mises stress experienced in the column during the tilting of the furnace
*Source: Own creation in Microsoft Excel 2016*

**Thanks**

The authors would like to thank the Tecnológico Nacional de México, which, through the Instituto Tecnológico de Morelia, provided financial support for the publication of this material.

**Conclusions**

With the analysis of the stress state strategically planned for the hydraulic cylinder-assisted joint system, the stability of the structures during the operation of high-risk displacement processes is guaranteed. In the example of the furnace with a maximum load of 4414.5 N (450 kg) per flank, a cylinder with a 2-inch diameter piston exceeds the maximum pressure of 248.11 psi since for each unit of power, there would be 3500 psi according to the manufacturer. The material of the IPS beam (ASTM A529 Grade 50) yield stress of 250 MPa would not present deformation during the work sessions.

**References**

Audet, D., Parent, L., Deveaux, M., & Courtenay, J. (2004). Aluminum Weighing Measurement in Tilting Furnaces. In TMS (Ed.), *Light Metals 2004* (pp. -). Charlotte, North Carolina: The Minerals, Metals & Materials Society.

Dadhania, N., Bhatiya, S., Joshi, A., & Sharma, D. (2016). Review of Cabin Tilting Mechanism for Earth-Moving Machinery. *International Journal Of Advance Research And Innovative Ideas In Education*, 510-514.

Dieter, E. G. (1986). *Mechanical Metallurgy*. McGraw-Hill Series in materials science and engineering.

Hu, J., Pan, J., Dai, B., Chai, X., Sun, Y., & Xu, L. (2022). Development of an Attitude Adjustment Crawler Chassis for Combine Harvester and Experiment of Adaptive Leveling System. *Agronomy, 12*(717), 1-16. doi:https://doi.org/10.3390/agronomy12030717

MIPSA. (2023, Julio 06). *Viga IPS (IS)*. Retrieved from MIPSA Expertos Procesando Metales: https://www.mipsa.com.mx/productos/acero/perfiles-estructurales/viga-ips-is/

ISSN 2523-6776

Nabertherm. (2023). *Furnaces for Foundry*. Lilienthal, Germany: Nabertherm GmbH. Retrieved from https://www.nabertherm.com/contacts

Nelson, E., Best, C., McLean, W., & Potter, M. (2010). *Schaum's Outline of Engineering Mechanics: Statics*. New York, Chicago, San Francisco, Lisbon, London, Madrid, Mexico City, Milan, New Delhi, San Juan, Seoul, Singapore, Sydney, Toronto: Schaum's McGraw-Hill Companies, Inc.

Sun, H., & Chiu, G. T.-C. (2001). Motion Synchronization for Multi-Cylinder Electro-Hydraulic System. *Proceedings of ASME 2001 International Mechanical Engineering Congress and Exposition* (pp. 1-11). New York: ASME.

Xu, J., & Yoon, H.-S. (2016). A Review on Mechanical and Hydraulic System Modeling. *Journal of Construction Engineering*, 1-11. doi:http://dx.doi.org/10.1155/2016/9409370

ISSN 2523-6776

Article **Journal of Technological Engineering**
December 2023, Vol.7 No.20 10-15

# Prediction model of a shell and tube heat exchanger based on the technique of artificial neural networks

# Modelo de predicción de un intercambiador de coraza y tubos basado en la técnica de redes neuronales artificiales

TORRES-RICO, Luis´*†, KOKU-TAMAKLOE, Elvis´, MANRÍQUEZ-PADILLA, Carlos´´ and VILLASEÑOR-AGUILAR, Marcos´´´,´´´´

´*Universidad Politécnica de Juventino Rosas, México.*
´´*Universidad Autónoma de Querétaro, México.*
´´´*Tecnológico Nacional de México/ITES de Irapuato, México.*
´´´´*Universidad Politécnica de Guanajuato, México.*

ID 1st Author: *Luis, Torres-Rico* / **ORC ID**: 0000-0002-6873-0363, **CVU CONAHCYT ID**: 373689

ID 1st Co-author: *Elvis Koku-Tamakloe*

ID 2nd Co-author: *Carlos G, Manríquez-Padilla* / **ORC ID:** 0000-0003-1332-5173, **CVU CONAHCYT ID:** 347939

ID 3rd Co-author: *Marcos, Villaseñor-Aguilar* / **ORC ID:** 0000-0003-0598-8145, **CVU CONAHCYT ID:** 294911

**DOI**: 10.35429/JTEN.2023.20.7.10.15 Received July 15, 2023; Accepted December 30, 2023

**Abstract**

The purpose of this paper is to report the proposal of a temperature prediction model methodology for a shell and tube heat exchanger using Artificial Neural Networks (RNAs). For the generation of the model, a set of historical data of five years was used, where 1633 readings from the equipment were obtained. The recorded data were the heat transfer coefficients and the fuel flow to predict the fluid temperature. The proposed methodology uses three stages. The first was the scaling of the data set between 0 and 1, this was done to facilitate the training of the RNA model: The second was to apply data mining techniques to create data clusters to model the behavior of the heat exchanger. The last stage was the evaluation of the prediction models. 5 proposals for Neural Network models were evaluated, these used 10 neurons in the hidden layer, the main difference between them was the number of clusters used in the training data that increased one by one. The average training errors obtained by the four types of data pools were 0.00220, 0.00190, 0.00133, 0.00098, and 0.00080. According to the results obtained, it was possible to conclude that the model that uses a greater number of clusters has a lower prediction error.

**Exchanger, Neural network, Flow**

**Resumen**

El presente trabajo tiene como finalidad reportar la propuesta de una metodología de modelo de predicción de temperatura de un intercambiador de coraza y tubos empleando Redes Neuronales Artificiales (RNAs). Para la generación del modelo se empleó un conjunto de datos históricos de cinco años donde se obtuvieron 1633 lecturas provenientes del equipo. Los datos registrados fueron los coeficientes de transferencia de calor y el flujo de combustibles para predecir la temperatura del fluido. La metodología propuesta utiliza tres etapas. La primera fue el escalamiento del conjunto de datos entre 0 y 1 esto se realizó para facilitar el entrenamiento del modelo de RNA: La segunda fue aplicar técnicas de minería de datos para crear agrupamientos de datos para modelar el comportamiento del intercambiador de calor. La última etapa fue la evaluación de los modelos de predicción. Se evaluaron 5 propuestas de modelos de Redes Neuronales estos emplearon 10 neuronas en la capa oculta, la principal diferencia de ellos fue la cantidad de clúster utilizados en los datos de entrenamiento que se fueron incrementando de uno en uno. Los errores promedios de entrenamiento obtenidos por los cuatro tipos de agrupamientos de datos fueron 0.00220, 0.00190, 0.00133, 0.00098 y 0.00080. De acuerdo a los resultados obtenidos se pudo concluir que el modelo que emplea mayor cantidad clúster tiene un error menor de predicción.

**Intercambiador, Red neuronal, Flujo**

**Citation:** TORRES-RICO, Luis, KOKU-TAMAKLOE, Elvis, MANRÍQUEZ-PADILLA, Carlos and VILLASEÑOR-AGUILAR, Marcos. Prediction model of a shell and tube heat exchanger based on the technique of artificial neural networks. Journal of Technological Engineering. 2023. 7-20:10-15.

* Correspondence to Author (E-mail: mvillasenor@upgto.edu.mx)
† Researcher contributing as first author.

 

## Introduction

Artificial Intelligence (AI) is a branch of computational science that has been used in modeling the behavior of industrial equipment and processes (Casteleiro-Roca, Barragan, Segura, Calvo-Rollea, & Andújar, 2019). This presents the advantage of facilitating the processing and treatment of the data that form the knowledge base of the system to be modeled (Wetenriajeng Sidehabi, Suyuti, Sari Areni, & Nurtanio, 2018). Furthermore, this has been used in different application models such as: heat exchangers, controllers and vision systems ( Villaseñor-Aguilar, Ramírez-Agundis, Padilla-Medina, & Orozco-Mendoza, 2011) ( Villaseñor-Aguilar, et al.

AI is divided into different branches such as fuzzy logic, genetic algorithms and expert systems (Ponce Cruz). Neural Networks allow mapping and modeling the behavior of the knowledge base associated with systems or processes without using their mathematical model. Its operation is focused on mapping input and output data, this is achieved by using a nonlinear processor called perceptron ( Villaseñor-Aguilar, Ramírez-Agundis, Padilla-Medina, & Orozco-Mendoza, 2011). This modifies its synaptic weights to provide the desired response as shown in Figure 1 (Villaseñor Aguilar , Montecillo-Puente, Obed-Noé, & López Enriquez, 2017). The synaptic weights are calculated by means of an ANN training algorithm (Vazquez-Cruz, Luna-Rubio, Contreras-Medina, Torres-Pacheco, & Guevara-Gonzalez, 2012) that learns the desired behavior from the knowledge base to predict variables such as: temperature, Nussult number and Reynolds number (Wang, Xie, Zeng, & Luo, 2006).

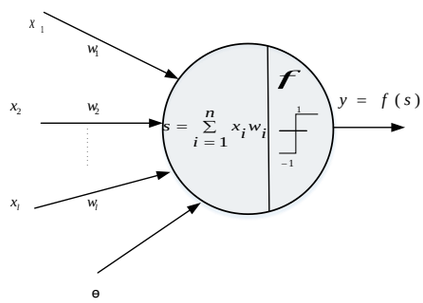


**Figure 1** Perceptron model: Xi input signals, Wi weights, S weighting of the perceptron, f activation function

(Wang, Xie, Zeng, & Luo, 2006) applied an ANN to the heat transfer analysis of a shell and tube heat exchanger. The output variables of their model were the outlet temperature difference on each side and the total heat transfer rates. (Duran, Rodriguez, & Airton Consalter, 2009) proposed a cost estimation model for shell and tube heat exchangers. (Anand, 2016) presented a comparison of four ANN configurations to calculate the outlet temperature. (Hemmat Esfe, 2017) designed an ANN to determine the heat transfer characteristics and pressure drops of nanofluids in a heat exchanger. (Zeeshan, Azmi Hazarika, Nath, & Bhanja, 2017) estimated the heat transfer performance of the exchanger, jointly reported an ANN that predicts the transfer coefficient, Nussult number and Reynolds number.

This work proposes a methodology that models the behavior of a shell and tube exchanger using a fluid and thermal properties. The objective of the research is to generate a proposal of heat exchanger prediction models based on the ANN technique. The proposed models can be used as a support tool for data reconstruction and support the solution of industrial problems.

## Description of the method

This section presents the methodology used for the development of the work. Figure 2 shows a flow diagram of the different stages used in the ANN-based model. The set of operating blocks of the model was developed in Matlab®. The first stage involved the selection of data that were complete in order to form the knowledge base, which were then normalized from 0 to 1. The next stage was responsible for varying the number of groups to be used for training the ANN. Subsequently, the ANN models were created using the Matlab® toolbox. The architecture used uses the fuel flow and the transfer coefficient as input, and the temperature as output. The next stage consisted of training the ANN models using 75% of the data and the rest was used for validation. During the training stage, the number of neurons contained in the hidden layer and the number of data sets were varied. The last stage consisted of selecting the ANN model with the lowest error.

ISSN 2523-6776

In the content of the article, all graphs, tables and figures must be editable in formats that allow modifying size, type and number of letters, for editing purposes, these must be in high quality, not pixelated and must be noticeable even if the image is reduced to scale.

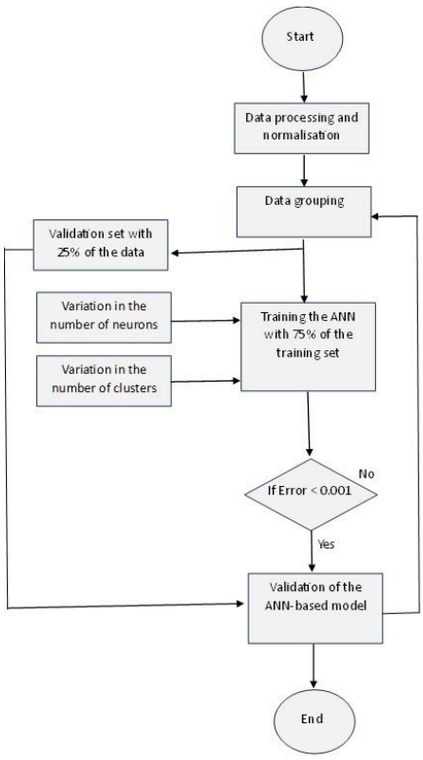


**Figure 2** Block diagram of the system developed in Matlab ®: a) User interface, b) Processing and treatment, c) Clustering module, d) ANN prediction system

*Data Collection*

The database provided was processed to select the modeling information. Two criteria were used. The first was to select the data where their information records were complete. The second was that the thermal change was fulfilled.

*Data processing and treatments*

The second block consists of forming the training set with completed records and scaled to a range of (0 to 1). The scaling is required as it facilitates the learning of the network. The recorded data are divided into two parts, the input data and the output data to the network. The input data corresponds to the fluid flow, coefficient and the output data consists of the output temperatures. Equation (1) was used to *perform the normalization*.

$$X_{normalzado} = \frac{X - X_{min}}{X_{max} - X_{min}} \quad (1)$$

*Clustering*

The third block, performed in the clustering of data using the K-means algorithm. For the development of the clustering, the Matlab® Statistics and Machine Learning toolbox was used. The K-means algorithm consists of establishing K centroids, then using each element of the database and positioning it in the nearest centroid. The next step is to recalculate the centroids of each cluster and redistribute the elements to their nearest cancroid. This process is repetitive until there are no variations in the centroids.

*ANN prediction system*

This section presents the methodology used for the development of the ANN. In addition, the training response of the neural network is analyzed by varying some of the characteristics, mainly the number of neurons in the hidden layer and the number of data sets. This is done in order to choose the best possible network configuration.

In the first phase of the development of the prediction system I used the whole training set. Using as inputs the fluid exchanger fluid and transfer coefficient as output fluid outlet temperature 1. Figure 3 shows the ANN architecture used for training without clustering in the inputs.

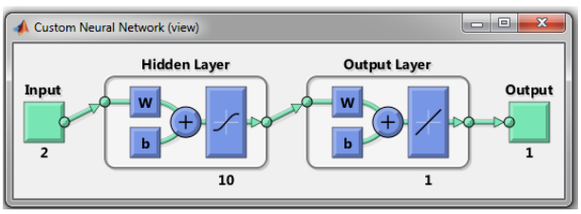


**Figure 3** ANN schematic of the proposed model without input clustering.

Table 1 shows the results obtained from the training of five proposed architectures for the temperature prediction model. The ANN of 10 neurons in both layers is the one that presented the lowest minimum error of 0.00187. The training of the ANNs was performed using the Matlab Neural Network Toolbox.®.

ISSN 2523-6776

| RNA | Inputs | Layer 1 | Layer 2 | Outputs | Error MSE |
|---|---|---|---|---|---|
| Model 1 | 2 | 10 | - | 1 | 0.00220 |
| Model 2 | 2 | 25 | - | 1 | 0.00205 |
| Model 3 | 2 | 10 | 10- | 1 | 0.00187 |
| Model 4 | 2 | 25 | 25- | 1 | 0.00197 |

**Table 1** Proposed models without input grouping

In Figure 4, the histogram of the ANN errors between the ANN output and the actual data is shown. The error interval is shown on the horizontal axis. The vertical axis shows the number of trials falling into a specific error interval. The amount of data used in the input and output training was 1706, with dimensionality 2 and 1, respectively.

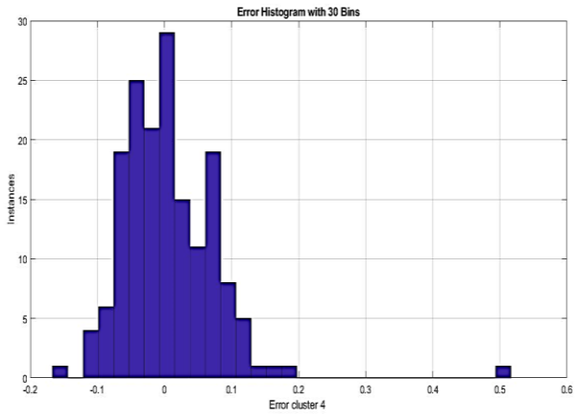


**Figure 4** Training error of the temperature prediction ANN. This histogram shows the errors of the output data together, 1x 17066 data

During the process of developing the prediction model, it was proposed to create several ANN models by clustering the data. Table 2 shows the errors of each ANN model using data clustering. All models used 2 inputs, 1 output and 10 neurons in both hidden layers. Subsequently, the average error of each cluster was determined to select which model presents the best response for training.

| RNA | Error Cluster 1 | Error Cluster 2 | Error Cluster 3 | Error Cluster 4 | Error Cluster 4 |
|---|---|---|---|---|---|
| Model 1 | 0.00180 | 0.00200 | - | - | - |
| Model 2 | 0.00199 | 0.00202 | 0.00183 | - | - |
| Model 3 | 0.00208 | 0.00187 | 0.00220 | 0.00167 | - |
| Model 4 | 0.00190 | 0.00210 | 0.00218 | 0.00190 | 0.00239 |

**Table 2** Proposed models with input grouping.

Table 3 shows that model 5 had the lowest average error of all the models.

| RNA | Cluster | Error average |
|---|---|---|
| Model 1 | 2 | 0.00190 |
| Model 2 | 3 | 0.00133 |
| Model 3 | 4 | 0.00098 |
| Model 4 | 5 | 0.00080 |

**Table 3** Average error of the proposed models with input clustering
*Source: Own elaboration*

## Results

The system predictions are shown in Figure 3 using the training set. Each figure describes the behavior of the data using the five clusters. The input variables are transfer coefficients corresponding to the x-axis, the y-axis the fluid flow and as a predicted variable the fluid outlet temperature is the z-axis.

However, pronounced variations can also be observed at some points; these could be reduced by training the ANN continuously using more recent data or by creating new clusters of information. After inputting the data to the prediction model, a mean square error of approximately 0.0005 was obtained. The error histograms for these data are shown in Figures 5-8

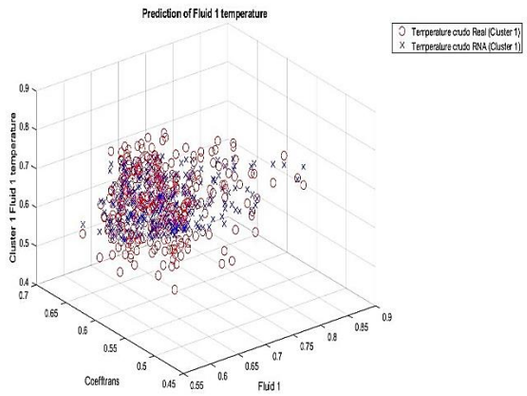


**Figure 5** Comparative plots of actual temperature vs. RNA temperature of cluster 1 (cluster 1)

ISSN 2523-6776

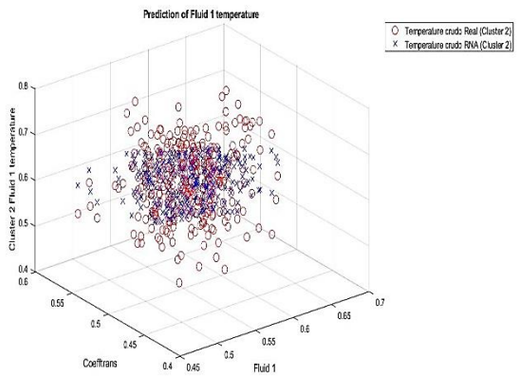


**Figure 6** Comparative plots of actual temperature vs. RNA temperature of cluster 2)

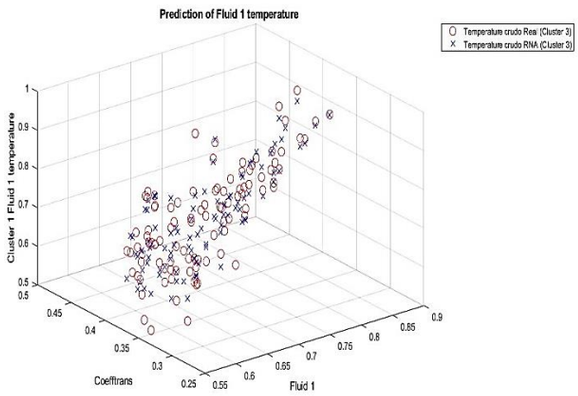


**Figure 7** Comparative plots of actual temperature vs. RNA temperature of cluster 3)

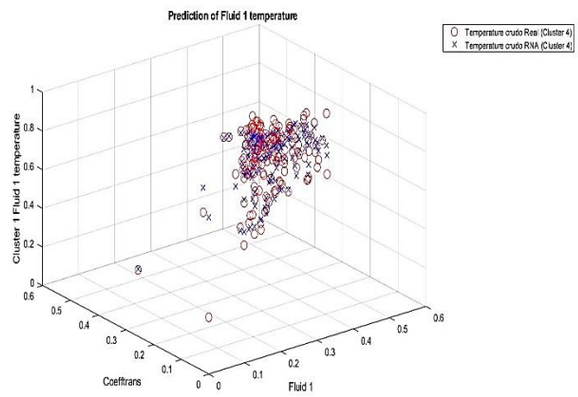


**Figure 8** Comparative plots of actual temperature versus RNA temperature of cluster 4

## Conclusions

It can be concluded that the application of the use of Artificial Neural Networks facilitates the modeling of complex systems such as heat exchangers.

In conjunction, it identified that the use of the K-means technique and the artificial neural network models present a good prediction of the temperature output and a small prediction error. An essential part of having a good shell and tube heat exchanger model is to have a good pooling of the training and log data.

## References

Villaseñor-Aguilar, M. J., Botello-Álvarez, J. E., Pérez-Pinal, F. J., Cano-Lara, M., León-Galván, M. F., Bravo-Sánchez, M. G., & Barranco-Gutierrez, A. I. (2019). Fuzzy classification of the maturity of the tomato using a vision system. Journal of Sensors, 2019. https://www.hindawi.com/journals/js/2019/3175848/ ,https://doi.org/10.1155/2019/3175848

Villaseñor-Aguilar, M., Ramírez-Agundis, A., Padilla-Medina, J. A., & Orozco-Mendoza, H. (2011). Control de estabilidad de un manipulador planar paralelo 3RRR utilizando redes neuronales. Científica, 15(3), 107-115., ISSN:1665-0654 https://www.redalyc.org/pdf/614/61420811002.pdf

Anand, M. (2016). Mid Term Electrical Load Forecasting for State of Himachal Pradesh using different weather conditions via ANFIS Model. https://www.researchgate.net/publication/331035621_Mid_Term_Electrical_Load_Forecasting_for_State_of_Himachal_Pradesh_using_different_weather_conditions_via_ANN_Model

Casteleiro-Roca, J.-L., Barragan, A. J., Segura, F., Calvo-Rollea, J. L., & Andújar, J. M. (2019). Sistema hıbrido inteligente para la predicción de tensión de una pila de combustible. Revista iberoamericana de automática e informática industrial ( RIAI ), ISSN-e 1697-7920, Vol. 16, Nº. 4, 2019, págs. 492-501https://dialnet.unirioja.es/servlet/articulo?codigo=7073777

Duran, O., Rodriguez, N., & Consalter, L. A. (2009). Neural networks for cost estimation of shell and tube heat exchangers. Expert Systems with Applications, 36(4), 7435-7440. https://doi.org/10.1016/j.eswa.2008.09.014

ISSN 2523-6776

Hemmat Esfe, M. (2017). Designing an artificial neural network using radial basis function (RBF-ANN) to model thermal conductivity of ethylene glycol–water-based TiO2 nanofluids. Journal of Thermal Analysis and Calorimetry. https://doi.org/10.1007/s10973-016-5725-y

Ponce Cruz, P. (s.f.). INTELIGENCIA ARTIFICIAL con aplicaciones a la ingenieria. Alfaomega.

Vazquez-Cruz, M., Luna-Rubio, R., Contreras-Medina, L., Torres-Pacheco, I., & Guevara-Gonzalez, R. (2012). Estimating the response of tomato (Solanum lycopersicum) leaf area to changes in climate and salicylic acid applications by means of artificial neural networks. Biosystems Engineering. https://doi.org/10.1016/j.biosystemseng.2012.05.003

Villaseñor Aguilar , M., Montecillo-Puente, F.-J., Obed-Noé, S.-A., & López Enriquez, R. (2017). Predicción de heladas en cultivos usando redes neuronales en la zona de Salvatierra Guanajuato. Revista Ingeniantes, 4(1), 1. https://citt.itsm.edu.mx/ingeniantes/articulos/ingeniantes4no1vol1/Prediccion%20de%20heladas.pdf

Wang, Q., Xie, G., Zeng, M., & Luo, L. (2006). Prediction of heat transfer rates for shell-and-tube heat exchangers by artificial neural networks approach. Journal of Thermal Science, 15, 257-262. https://doi.org/10.1007/s11630-006-0257-6

Wetenriajeng Sidehabi, S., Suyuti, A., Sari Areni, I., & Nurtanio, I. (2018). Classification on passion fruit's ripeness using K-means clustering and artificial neural network. 2018 International Conference on Information and Communications Technology (ICOIACT). DOI: 10.1109/ICOIACT.2018.8350728

Zeeshan, M., Azmi Hazarika, S., Nath, S., & Bhanja, D. (2017). Numerical investigation on the performance of fin and tube heat exchangers using rectangular vortex generators. AIP Conference Proceedings. https://doi.org/10.1063/1.4990164

ISSN 2523-6776

Article **Journal of Technological Engineering**
December 2023, Vol.7 No.20 16-25

# Frutty-Pi (fruit sorter)

# Frutty-Pi (clasificador de frutas)

CORTES-GARCIA, Alicia†*, VALENCIA-GARCIA, Cesar Alejandro, SANTOS-OSORIO, Rene and RODRIGUEZ-MIRANDA, Gregorio

*Universidad Tecnológica de San Juan del Río, México.*

ID 1st Autor: *Alicia Cortes García* / **ORC ID:** 0000-0003-1044-9787, **CVU CONAHCYT ID:** 671816

ID 1st Co-author: *Alejandro Cesar Valencia García* / **ORC ID:** 0000-0002-6671-7915, **CVU CONAHCYT ID:** 671805

ID 2nd Co-author: *Rene Santos Osorio* / **ORC ID:** 0000-0002-4411-7628, **Thomson ID Research:** G-3453-2019, **CVU CONAHCYT ID:** 619722

ID 3rd Co-author: *Gregorio Rodríguez Miranda* / **ORC ID:** 0000-0002-2512-892X, **Publons ID:** S-5808-2018, **CVU CONAHCYT ID:** 246718

**DOI:** 10.35429/JTEN.2023.20.7.16.25 Received July 20, 2023; Accepted December 30, 2023

**Abstract**

Currently, the inventory management in the IT area is handled with an existing software which not only works as inventory, but also is a responsive generator which is used when equipment is delivered to the user by IT. The software needed improvements that were necessary to continue with its use, this because there are things that do not like the administrators who only have access to that database IT staff of the company GG Cables and Wires Mexico S. De R.L de C.V. For this work was made the call for an intern who could do that job. We were making use of Visual Basic code, so we continued using it to make the necessary corrections so that the software was working in a better way. All this in order to have a better way of use and an improvement in the file management system in order to manage a control by areas with the responsives in a digital way.

**Digital, Software, File management**

**Resumen**

Actualmente, el manejo de inventario en el área de IT se maneja con un software existente el cual no solo funciona como inventario, sino que también es un generador de responsivas el cual las responsivas se utilizan cuando se le hace entrega de equipo entregado a Usuario por parte de IT. El software necesitaba de mejoras que eran necesarias para poder continuar con su uso, esto debido a que hay cosas que no gustan a los administradores el cual solo tienen acceso a esa base de datos personal de IT de la empresa GG Cables and Wires México S. De R.L de C.V. Para este trabajo se hizo la convocatoria de un practicante el cual pudiera realizar ese trabajo. Se estaba haciendo uso de código en Visual Basic por lo cual se continuó haciendo uso de él y así mediante ese código realizar las correcciones necesarias para que el software estuviera funcionando de una mejor forma. Todo esto con la finalidad de contar con una mejor forma de uso y una mejora en el sistema de gestión de archivos para así manejar un control por áreas con las responsivas de manera digital.

**Digital, Software, Gestión de archivos**

**Citation:** CORTES-GARCIA, Alicia, VALENCIA-GARCIA, Cesar Alejandro, SANTOS-OSORIO, Rene and RODRIGUEZ-MIRANDA, Gregorio. Frutty-Pi (fruit sorter). Journal of Technological Engineering. 2023. 7-20:16-25.

† Researcher contributing as first author.

 

## Introduction

The project is carried out in the subject of Internet of Things (IoT) at the Technological University of San Juan del Rio (UTSJR), the activity is the final project of the degree of University Technician so it involves the integration of multiple subjects and technologies for its conclusion. The topic was chosen due to the interest in testing artificial intelligence in the field of microcontrollers such as raspberry-pi and Arduino, in addition to the interest in image analysis from artificial intelligence was another of the most important factors in determining where the project would focus.

The objective planned with this project is to create a vegetable classifier in which with 2 cameras and the help of AI will register each of the vegetables and the state in which they are.

With this we plan to help companies that are engaged in the sale of vegetables or farmers to classify in a simpler way each vegetable and increase production in a more efficient way for them.

*Company background*

The Technological University of San Juan del Rio, is a Higher Education Institution created in August 1998, which offers young high school graduates, university careers closely linked to the productive sector so that in a short term they can be incorporated into the professional work of the region. Our main objective is to achieve an integral quality education, according to our Quality Management System, so that our students have solid knowledge, practical experience, attitudes and values.

Its vision is to form people with integrity in higher education, through a culture of scientific and technological development and social responsibility, offering quality technological services, through a close link with the different sectors, with the ability to adapt to the environment.

It also seeks to be a global university, a reference of innovation, recognized for the quality of its educational and technological services, the competitiveness of its graduates and its transcendence in the generation and application of knowledge.

The Universidad Tecnológica de San Juan del Río undertakes a Feasibility Study in conjunction with municipal presidents, prominent members of society and local businessmen, from the municipalities of Jalpan de Serra, Pinal de Amoles, Landa de Matamoros and Arroyo Seco; which results in the creation of the Academic Unit of Jalpan de Serra of the UTSJR.

In this way we intend to contribute to the economic development of the region, from the neuralgic point of the area, with technological education that promotes the development of local companies and the creation of micro-enterprises that rationally exploit the vast resources of the region and are responsible with the environment.

## Problem Statement

Fruit or vegetable sorting with AI and raspberry PI.

## Justification

Fruits and vegetables in bad condition are always a problem when it comes to selecting our food, besides they represent a risk for clueless people who add them to their meals, this is why we thought of eliminating this problem before it arrives to our trusted greengrocers. We plan to do this with our invention.

## Overall objective

The objective planned with this project is to create a vegetable sorter in which with 2 cameras and the help of AI will register each of the vegetables and the state they are in.

With this we plan to help companies that are dedicated to the sale of vegetables or farmers to classify in a simpler way each vegetable and increase production in a more efficient way for them.

## Scope

Create a vegetable sorter, with the resources of each of the team members, and also for final delivery a fully functional machine that will probably be used in a small greenhouse to optimize the collection and sorting of the products generated, with a delivery date of 30/03/2023.

ISSN 2523-6776

**Theoretical framework**

*Raspberry*

It is a low-cost computer with a compact size, the size of a credit card, can be connected to a computer monitor or a TV, and used with a standard mouse and keyboard. It is a small computer running a Linux operating system capable of allowing people of all ages to explore computing and learn programming languages such as Scratch and Python. It is capable of doing most of the tasks typical of a desktop computer, from browsing the internet, playing high-resolution videos, manipulating office documents, to playing games. (PI, 2018, p. 1)

It serves to bring computing to everyone, with it you can perform the most common tasks of a computer, but for only an approximate price of $ 35, with a Raspberry Pi and a Raspbian system you can browse the internet, check email, play videos, use instant messaging applications, etc.. All this in a very small size and at a much lower cost than any other desktop computer (PI, 2018, p. 1).

I wanted to bring computing to all users, with this simple board, but enough to do the most common tasks of any computer, computing is within the reach of all users and even pockets. It has also been introduced for teaching computer science in schools, it can be purchased in batches for the education sector from its own website that will redirect us to the partner distributor for this. (Delgado, 2018, p. 1)

*Artificial intelligence*

AI can be defined as the ability of computers to do activities that normally require human intelligence. But, to provide a more detailed definition, we could say that AI is the ability of machines to use algorithms, learn from data, and use what they learn in making decisions just as a human would. However, unlike people, AI-based devices do not need to rest and can analyze large volumes of information at a time. Also, the error rate is significantly lower in machines performing the same tasks as their human counterparts. (Rouhiainen 17)

Performance improvements of algorithmic trading strategy: it has already been implemented in various ways in the financial sector.

- Efficient and scalable processing of patient data: this will help make medical care more effective and efficient.

- Predictive maintenance: another tool widely applicable in different industrial sectors.

- Object detection and classification: this can be seen in the autonomous vehicle industry, although it also has potential for many other fields.

- Content distribution on social networks: this is primarily a marketing tool used in social networks, but can also be used to raise awareness among non-profit organizations or to disseminate information quickly as a public service.

- Protection against cybersecurity threats: it is an important tool for banks and systems that send and receive online payments. (Rouhiainen 18)

Machine learning is one of the main approaches to artificial intelligence. Simply put, it is an aspect of computer science in which computers or machines have the ability to learn without being programmed to do so. A typical result would be suggestions or predictions in a particular situation (Rouhiainen 19).

To begin to reflect on the great impact that AI will have on our lives, it is useful to know that AI technologies have begun to develop the ability to see (machine vision), hear (speech recognition) and understand (natural language processing) as never before. Figure 1.4 clearly illustrates this concept. Previously, these abilities belonged only to humans, but in the near future machines and robots will be able to develop them thanks to AI. (Rouhiainen 23)

A well-known phrase often heard in the technology community is that "data is the new oil," a famous quote originally attributed to British mathematician Clive Humby. Today, the most powerful companies in the world are often those that have access to vast amounts of data. But it is also worth noting that it is not only the volume of data that matters in business, but also the quality. Personally, however, I would argue that data is even better than oil. In the years when it was one of the world's most valuable commodities, only a few companies could enjoy its benefits.

ISSN 2523-6776

Today, however, because almost anyone can learn the basics of AI and machine learning, using these skills to create valuable tools and having access to free online data sources with ease is a new scenario where everyone will be able to benefit from it. (Rouhiainen 25)

**Fruit maturity**

The concept of fruit processing is understood within the agricultural market as a set of processes applied to fruit, namely cooling and ripening (Velez and Velez 27).

Fruit may have different degrees of maturity, depending on the type of fruit (Gueche G. C., 2020). The grade of the fruit will always be required by the client, in this case the exporters and suppliers of traditional fruits (Velez and Velez 27).

Traditional fruit exporters mostly trade with fruit processors. This is done in orders with very specific specifications, such as: temperature, number of batches, day of delivery and degree of ripeness of the fruit. (Velez and Velez 28)

The exporting entity named Congelados Ecuatorianos ECUACONGELA S.A., RUC 0992135948001, has the mission of exporting and supplying traditional fruit. This entity has methods and tools for the identification of maturity grades. One of the fruits supplied by this plant is the banana, which, by the way, is the fruit that will be taken as a case study (Velez and Velez 29).

**3D Printing**

3D printing is the process of creating objects by depositing layers of material on top of each other. 3D printing is referred to as additive manufacturing (AM) instead of traditional subtractive methods, such as CNC milling, when used for industrial production.

The technology has been around for about four decades, invented in the early 1980s. Although 3D printing started out as a slow and expensive technique, extensive technological advances have made today's AM technologies more affordable and faster than ever. ("3D Printing, what is it and how does it work? "1)

When we talk about 3D printer filaments, we are referring to the raw material used to produce the designs. To better understand, this element is similar to the paper used in conventional printers. (Otero 2022, 1)

The uses of 3D printing have increased considerably in recent times. Although we have already hinted at some of them in the introduction to this article, the list of applications is really long. Three-dimensional printers are useful in:

- Medicine. Printing of prostheses, organs or transplants.
- Automotive. Parts for cars and other means of transportation.
- Industry. Product development in industries for different types of businesses.
- Food printing. Obtaining various foods by three-dimensional printing.
- Others. 3D printers have become very recurrent devices in educational centers or in architecture studios.(Otero 2022 1)4

**Cameras on Raspberry PI**

Adding an "eye" to your Pi is a fantastic way to turn your board into a surveillance camera or a PC that can be used for video chatting. For this purpose, you can opt for compatible camera modules, or you can opt for an HD camera from an established brand, such as Logitech. These devices capture high-definition images and can also record videos for later viewing (" Raspberry Pi cameras Everything you need to know"). RPi camera modules use the special MIPI CSI camera format to use less power, enable faster bandwidth and fit a smaller physical size. In addition, these modules support higher resolution, better frame rate and have reduced latency issues compared to USB cameras (" Best Raspberry Pi Cameras Everything You Need to Know").

*React JS*

React JS is one of the most popular JavaScript libraries for mobile and web application development. Created by Facebook, React contains a collection of reusable JavaScript code snippets used for building the user interface (UI) called components ("React," 2020, pg 1).

ISSN 2523-6776

To understand how React works it is key that we place ourselves in context, because when you learn web development you gain knowledge of three basic concepts:

- HTML: the semantics, structure and information of the web page; that is, its skeleton.
- CSS: the appearance of our web page.
- JavaScript: basically the brain of our page. It determines what to do based on what happens on it (React App,2020, pg 1).

*AI Training*

Artificial Intelligence (AI) training is the foundation on which the project rests, so it is our first aspect to discuss. This training is carried out in a total of 3 phases, being these collect samples, model preparation and model export, each with its own processes and unique ways of working, below is shown in a more detailed way each of the phases exposed above, this whole process was carried out with the Google Teachable Machine tool.

**Sample collection**

This phase consists of collecting and grouping the examples you want the computer to learn by classes or categories. Each class or category will represent an object or element that the artificial intelligence must learn separately, in this case and taking this phase in the context of our project we have created a total of 6 classes, i.e. 2 classes for each fruit depending on its state (fresh or rotten).

The samples are each of the images that will be stored in the categories, on average each category has a total of 1800 photos that were collected from the internet and sometimes even taken by us personally.

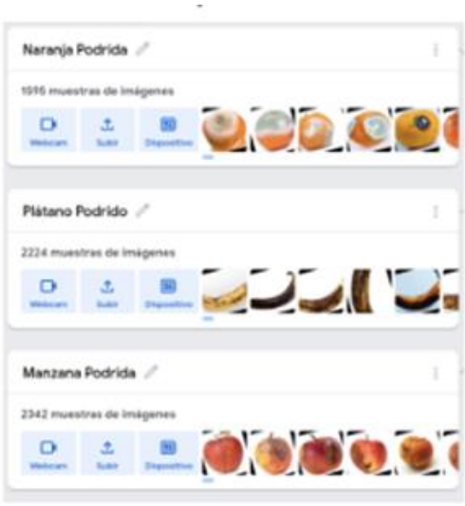


**Figure 1** Fruit model 1

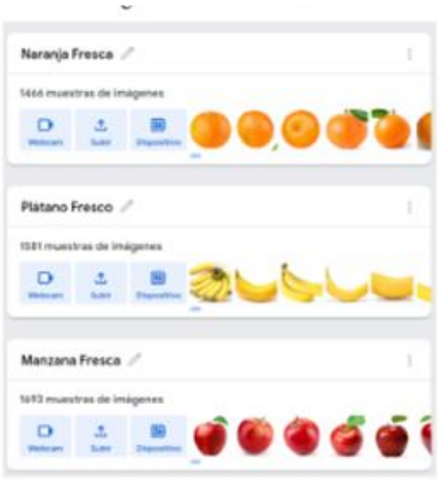


**Figure 2** Fruit model 2

The wide variety of images allows us to create a model that predicts much better the multiple environments that can be presented throughout its operation, it is more than clear that it will not always be used under the same conditions.

**Model preparation**

Prepare the model and test it on the fly to see if it can correctly classify the new examples. In this phase we must take care of 3 aspects that directly influence the result that our model will return, these aspects are: Epochs, batch size and learning rate.

Epochs: When the preparation model has processed all the samples of the preparation data set once, it is said that an epoch has been completed.

ISSN 2523-6776

For example, if 50 epochs are set, the model you are preparing processes the entire preparation data set 50 times. Generally, the larger the number, the better the model will learn to predict the data.

Batch size: A batch is a set of samples that are used in a preparation iteration. For example, let's say you have 80 images and you choose a batch size of 16. This means that the 80 images will be divided into batches of 16, resulting in 5 batches. When the model processes all 5 batches, an epoch will be completed.

The learning rate: Be careful when changing this number! Even the smallest differences can greatly influence the learning efficiency of your model. The settings of all these parameters will determine the quality of the training and how successful the model will be, you have to be careful with the selected values as they determine how long the training will take.

In our case the selected configuration was:

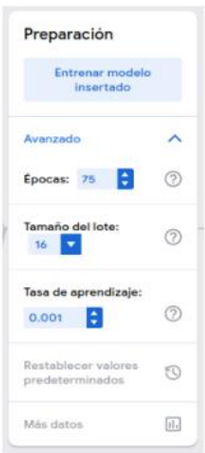


**Figure 3** AI training

It should be noted that we did not reach this conclusion from the first iteration, as we needed multiple tests to find the perfect combination.

*Export*

Export your model for your projects: sites, applications and more. We can download the model or host it online. These are one of the many advantages of using the Teachable Machine tool.

*Web Application*

However to have a complete project it is necessary to find a way to integrate all our subjects to get the best possible result, that's why it is called an integrative project, in this section we will discuss a little about the web application that we decided to create in order to manage our project from other perspectives.

The operation of the application is summarized in a place where we can observe the information generated by the model in a more intuitive and friendly way, which makes it available for anyone to generate a report with the information it provides.

*Interface*

The application has a friendly interface for the user in which you can register and with the username and password that you put log in whenever you want, this interface is created so that you can consult the information of the fruits that are stored in the database.


**Figure 4** Login app

*Libraries*

Different libraries were used in order to be able to use code that helped us in the creation of the application, since functions such as being able to use the camera to detect our fruits and compare the images with those in the model of each fruit are required.

*Operation*

The main objective of this web application is to show the user already registered, the fruits that have been registered in graphs that will be displayed according to the selected day. This graph will show the fruits divided in jars and in rotten making the sum of these fruits depending on which one is and the state of the same one.

ISSN 2523-6776

*Server*

The server is the one that will be processing the information that the client sends as its user at the moment that the user registers, at the same time that when the fruit is entered it will be sent through the client and the server processes it to save it in the database.

**Figure 5** Server 1

**Figure 6** Server 2

*Client*

It is the one that will be sending all the information to the server so that it processes it in the database and returns the functions that the client requested to the server socket, as its registration, the fruits that the client verifies in the classifier.

**Figure 7** Client 1

**Figure 8** Client 2

*Fruit Web Analyzer*

This script contains all the code for the identification of the fruits themselves, as we can see there are several lines of code for what is the api of teachable machine for the use of the images of the fruits.

**Figure 9** Teachable machine script

*Camera image script*

The script was made so that the camera can be used with the code and it collected the data sent to make the comparison with the teachable machine images.

**Figure 10** Camera script

ISSN 2523-6776

*Image comparison*

The script was created to compare the image that is being transmitted in the camera with the images of the model of each fruit, whether fresh or rotten, this is done through an if and else if condition that with a link will tell us which fruit is and if it is in good condition or rotten.

**Figure 11** Image comparison

*Online fruit analyzer*

In this page the fruit is analyzed and with the script is compared saying in the box on the right that fruit is and its state of the same, also sending the data of the compared fruit in the database that soon you can consult in the project page.

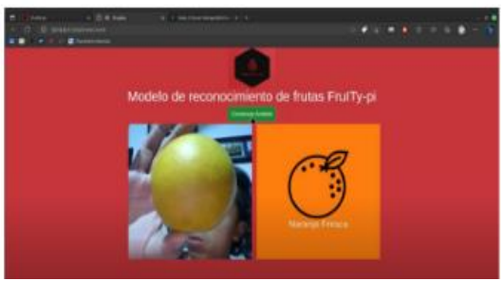


**Figure 12** Fruit analyzer

*Assembling the fruit sorter*

On the table you will place the box where the fruit will be placed, then you will need some lighting for detection, finally you will place the camera in such a way that the camera only shows the base of the box, not the walls of the same with this would be mounted what is the space where the main procedure will be done.

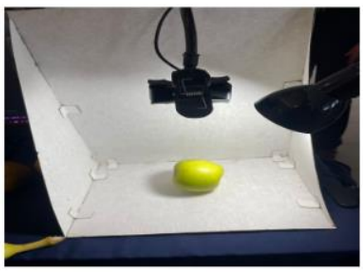

**Figure 13** Assembly 1

For the operation of the model will need 1 raspberry and two computers in the raspberry will run the server which receives all the data from the model and performs the analysis and generates statistics in the first computer runs the recognition model which is the one that sends the data and the last computer runs the web page which takes the data from the server.

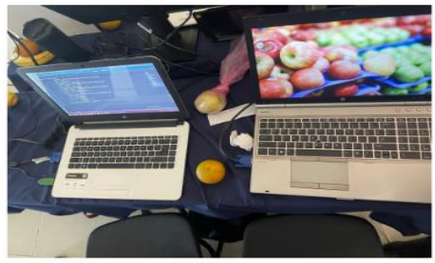

**Figure 14** Assembly 2

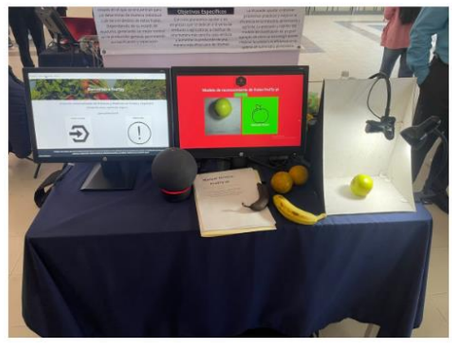

**Figure 15** Assembly 3

Here you can see the project completely assembled, where you can see two monitors, one shows the commercial of the product in which it is superficially explained what the project consists of and the other monitor shows the program already running.

## Results

The fruit classification model trained by artificial intelligence can be able to classify fruits at different stages of ripeness with high accuracy, using a wide variety of training images. The accuracy of the model can be measured by the percentage of correct classification on a test data set.

In addition, the speed and efficiency of the model can be improved by optimizing the algorithm and choosing appropriate model parameters. An efficient fruit sorting model can process a large amount of fruits in a short period of time, which can significantly improve productivity and efficiency in the food and agricultural industry.

ISSN 2523-6776

Overall, the results of the fruit sorting project can be highly accurate and efficient, which can have a positive impact on the industry and society.


**Figure 16** Analyzer Result

*Benefits*

This project can have several benefits, including:

- Increased accuracy in fruit sorting: AI can be trained to sort fruits by ripeness with high accuracy, which reduces the likelihood of human error and increases efficiency in the fruit sorting process.
- Improved product quality: By sorting fruits by ripeness stage, it can ensure that the products are of high quality and at their optimum ripeness, which can improve the quality and taste of the products.
- Reduced food waste: Accurate sorting of fruits by ripeness can reduce food waste, as fruits can be sorted and used at the right time for consumption or processing.
- Increased efficiency in the supply chain: Quick and accurate sorting of fruits by ripeness can improve efficiency in the supply chain, which can reduce costs and increase productivity.
- Technological innovation in the food industry: The use of artificial intelligence to sort fruits by ripeness is an innovative application of technology in the food industry, which can open up new opportunities for the development of technological solutions in the industry.

*Improvements*

The following are some improvements that can be considered for the project:

- Increase the diversity of training data: The AI model needs to be trained with a wide variety of images of different types of fruits and at different stages of ripeness, to improve its classification accuracy.
- Incorporating additional information: In addition to images, incorporating additional information such as texture, size, weight, and color of fruits can be considered to improve the accuracy of the classification model.
- Optimize the neural network: Optimization of the neural network and proper selection of hyperparameters can improve the accuracy and efficiency of the classification model.
- Use image preprocessing techniques: Applying image preprocessing techniques such as normalization, cropping, and denoising can improve the quality of the images and thus improve the accuracy of the model.
- Cross-validation: cross-validation can be considered to assess model accuracy and avoid over-fitting.
- Integrating technology with automation systems: Integrating the grading model with automation systems for fruit sorting and packing can improve efficiency in the supply chain and reduce human error.

## Conclusions

In conclusion, the fruit classification model trained using artificial intelligence has the potential to be highly accurate and efficient in classifying fruits at different stages of ripeness. The accuracy of the model can be measured using the percentage of correct classification on a test data set. In addition, optimization of the algorithm and proper choice of model parameters can improve its speed and efficiency.

The benefits of this project are diverse. First, higher accuracy in fruit classification is expected, which would reduce human errors and improve efficiency in the selection process. This would lead to an improvement in product quality, as fruits would be sorted at their optimum point of ripeness.

ISSN 2523-6776

Also, accurate sorting of fruits by ripeness would contribute to the reduction of food waste by using fruits at the right time for consumption or processing. In addition, efficiency in the supply chain would be increased through fast and accurate sorting, leading to reduced costs and increased productivity. Finally, this project represents a technological innovation in the food industry by applying artificial intelligence to sort fruits, opening new opportunities for the development of technological solutions in this field.

To improve this project, some improvements can be considered. First, it is important to increase the diversity of the training data, including images of different types of fruits and at different stages of ripeness, to improve the accuracy of the model. In addition, incorporating additional information, such as fruit texture, size, weight, and color, can be considered to further improve the classification accuracy. Optimization of the neural network and proper selection of hyperparameters can also contribute to improving the accuracy and efficiency of the model. The application of image preprocessing techniques, such as normalization, cropping, and denoising, can improve image quality and thus model accuracy. Cross-validation can be used as an additional strategy to assess model accuracy and avoid over-fitting. Finally, integration of fruit sorting technology with automation systems in the supply chain can increase efficiency and reduce human errors in fruit sorting and packing.

## References

Impresión 3D, ¿qué es y cómo funciona? (n.d.). Dassault Systèmes. Retrieved March 13, 2023, from https://www.3ds.com/es/make/guide/process/3d-printing

【Las mejores cámaras Raspberry Pi 】Todo lo que debes saber. (n.d.). Hazlo Linux. Retrieved March 13, 2023, from https://hazlolinux.com/raspberry-pi/las-mejores-camaras-raspberry-pi/

Otero, E. (2022, March 6). Filamentos para impresora 3D: qué son y para qué sirven. Profesional Review. Retrieved March 13, 2023, from https://www.profesionalreview.com/2022/03/06/filamentos-para-impresora-3d-que-son-y-para-que-sirven/

¿Qué es React JS y cómo funciona? (n.d.). Next U. Retrieved March 14, 2023, from https://www.nextu.com/blog/que-es-react-js-como-funciona-rc22/

React. (2020). Retrieved 03 14, 2023, from https://es.reactjs.org/

Rouhiainen, L. (2018). Inteligencia artificial: 101 cosas que debes saber hoy sobre nuestro futuro. Alienta Editorial. Retrieved March 13, 2023,from https://static0planetadelibroscom.cdnstatics.com/libros_contenido_extra/40/39308_Inteligencia_artificial.pdf

Velez, J. L., & Velez, N. A. (2021). DISEÑO E IMPLEMENTACIÓN DE UN SISTEMA DE CLASIFICACIÓN DEL GRADO DE MADUREZ DE UNA FRUTA.

ISSN 2523-6776

Article **Journal of Technological Engineering**
December 2023, Vol.7 No.20 26-39

# Photovoltaic system design for electrical supply in a parking lot

# Diseño de un sistema fotovoltaico para suministro eléctrico en un aparcamiento

ESCOBEDO-MARQUEZ, Diana Laura†, PALACIO-SIFUENTES, David Isaac, CASTILLO-CAMPOS, Nohemí Alejandra and ÁLVAREZ-MACÍAS, Carlos*

*Tecnológico Nacional de México / Instituto Tecnológico de la Laguna. C.P. 27000, Torreón, Coahuila, México.*

ID 1st Author: *Diana Laura, Escobedo-Márquez* / **ORC ID:** 0009-0005-9859-8251, **CVU CONAHCYT ID:** 1188232

ID 1st Co-author: *David Isaac, Palacio-Sifuentes* / **ORC ID:** 0009-0009-7454-5808, **CVU CONAHCYT ID:** 1305504

ID 2nd Co-author: *Nohemi Alejandra, Castillo-Campos* / **ORC ID:** 0009-0001-2490-4325, **CVU CONAHCYT ID:** 1271718

ID 3rd Co-author: *Carlos, Álvarez-Macías* / **ORC ID:** 0000-0002-2263-0316, **CVU CONAHCYT ID:** 165872

**DOI:** 10.35429/JTEN.2023.20.7.26.39 Received July 25, 2023; Accepted December 30, 2023

**Abstract**

Proposing new projects to boost photovoltaic solar energy can open opportunities to harness a free and virtually inexhaustible source like the sun, especially in countries such as Mexico where solar resources are among the most abundant on Earth's surface. In this chapter, a proposal for photovoltaic sizing was developed to supply energy to the buildings in the graduate studies area of the Instituto Tecnológico de la Laguna, located in Torreón, Coahuila. An analysis of the total estimated electrical consumption of these buildings was conducted to justify the installation of the photovoltaic system. Two proposals for photovoltaic sizing were presented, utilizing different inverter technologies. A 3D model was created using "Sketchup" to simulate the system installation. Costs and return on investment for the proposed project were also estimated. The results demonstrated that the use of central inverters was more cost-effective than the use of microinverters.

**Solar parking, Photovoltaic installation, Solar energy**

**Resumen**

Proponer nuevos proyectos que impulsen la energía solar fotovoltaica puede abrir oportunidades para aprovechar una fuente gratuita y prácticamente inagotable como el sol en países como México donde el recurso solar es uno de los mas abundantes en la superficie terrestre. Es presente trabajo presenta la propuesta de un estacionamiento fotovoltaico interconectado a la red en el Instituto Tecnológico de la Laguna que, además de generar energía eléctrica, proteja los automóviles de las intensas radiaciones que se viven en la zona. Para este trabajo se realizó un análisis del consumo eléctrico total estimado de los tres edificios para comparar la energía consumida con la energía generada. Se presentaron dos propuestas de dimensionado fotovoltaico utilizando diferentes tecnologías de inversores. Se creó un modelo en 3D utilizando el programa "Sketchup" para simular la instalación del sistema. También se estimaron los costos y el retorno de inversión del proyecto pensado para el 2023. Los resultados mostraron que el uso de inversores centrales resulta más económico que el uso de microinversores.

**Estacionamiento solar, Instalación fotovoltaica, Energía fotovoltaica**

**Citation:** ESCOBEDO-MARQUEZ, Diana Laura, PALACIO-SIFUENTES, David Isaac, CASTILLO-CAMPOS, Nohemí Alejandra and ÁLVAREZ-MACÍAS, Carlos. Photovoltaic system design for electrical supply in a parking lot. Journal of Technological Engineering. 2023. 7-20:26-39.

* Correspondence from the Author (E-mail: calvarezm@correo.itlalaguna.edu.mx)
† Researcher contributing as first author.

 

## Introduction

Due to the great potential of photovoltaic generation that Mexico has due to its high levels of radiation compared to other countries, the idea of proposing new projects that enhance the presence of photovoltaic solar energy can generate a niche of opportunities for energy use with a free and relatively inexhaustible source such as the sun. In addition, taking advantage of and promoting the consumption of these technologies reduces their price, making their application and manufacture more viable in the long term.

The Instituto Tecnológico de la Laguna located in Coahuila, Mexico, houses a large number of students and professors, which results in the provision of large areas for the parking of vehicles, however there are few areas of these that contemplate shading for vehicles as a necessity. The purpose of this work was to design a parking lot that takes advantage of the area of the photovoltaic modules while producing photovoltaic electrical energy that subsidizes a small fraction of the energy consumed by the university. This work contemplates the provisions of NOM-001-SEDE-2012, especially section 690 related to photovoltaic installations.

In this work, the processes, calculations and factors to be considered for the dimensioning of a photovoltaic array designated to a specific and limited area are proposed. In the same way, the sizing process will be carried out using two different current conversion technologies (specifically central inverters and microinverters) in order to discuss their differences, advantages, disadvantages, and propose an optimal model that fits the needs and facilities of the arrangement. In the same way, several models for the arrangement of the modules of the array were analyzed and their advantages and disadvantages were discussed. Finally, an approximate estimate of the dimensions made in this chapter was made, as well as a model made in "Sketchup" to have a better perception of the real dimensions of the installation.

## General concepts

In order to understand the elements that make up a photovoltaic array as well as its operation and the geographical and environmental factors that influence its performance, they will be described in this section as a theoretical framework.

*Solar resource in Mexico*

Mexico has great potential in terms of solar resources, so much so that UNAM (Universidad Nacional Autónoma de México) has highlighted the fact that using only 0.15% of the national territory (approximately 50 $km^2$) as a photovoltaic generation plant could receive enough solar radiation to meet the consumption needs of a population of 120 million inhabitants [1]. Due to the country's geographical position, it has great potential for harnessing solar radiation (Figure 1), leaving the country in a good position for the transition to the use of clean energy, specifically solar energy [1].

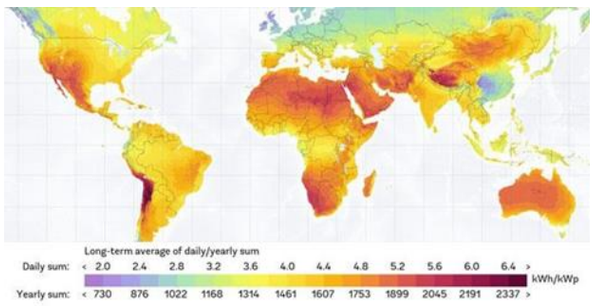


**Figure 1** Global radiation map
*Source: http://www.gisandbeers.com/cartografia-de-radiacion- solar-mundial/*

Encouraging the use of clean energy for electricity production has become a fundamental part of the fight against climate change around the world. Photovoltaic energy, on the other hand, has a great place in Torreón, Coahuila, due to its high levels of solar radiation that it receives daily, due to the fact that it is located near the western part of the country, where a greater amount of radiation is received per square meter (Figure 2) [1]. One of the advantages of photovoltaic energy is that it does not depend on large complex infrastructures such as combined cycle plants, which allows them to be small and minimally invasive. This has made it possible to develop projects where photovoltaic energy systems, especially the modules that make them up, serve a purpose other than producing electricity [2].

ISSN 2523-6776


**Figure 2** Map of Mexico with distribution of the municipalities with the highest radiation
*Source: https://solargis.com/es/maps-and-gis-data/download/mexico*

Over the years, various innovative ideas have emerged to apply photovoltaic technologies, such as solar chargers for mobile devices, their implementation in aeronautics and public lighting. Among the most outstanding proposals in the field of photovoltaic solar energy is the use of space through the installation of modules with additional functions. For example, photovoltaic parking lots are a promising concept, where the modules not only generate energy, but also provide cover for cars, protecting them from solar radiation, dust, snow, rain or hail (Figure 3) [3].

This dual-functionality approach not only contributes to the generation of clean energy, but also optimizes the use of space, providing additional benefits in terms of comfort and protection. These urban implementations of solar PV demonstrate how innovation in the design and integration of renewable technologies can generate practical and sustainable solutions to everyday needs.

**Figure 3** Examples of photovoltaic parking lots
*Source: https://www.syscomblog.com/2023/03/que- es-un-toldo-solar-una-decision.html).*

*Components of photovoltaic systems*

As in a human body, a photovoltaic system is made up of several individual parts that perform a separate task, but together they perform the task of transforming solar radiation into consumable electrical energy. The main element of a photovoltaic system is the solar cell, or photovoltaic cell and this is the primary component and smallest unit element of a photovoltaic module (MFV), and the set of interconnected photovoltaic modules is known as a line or "string" of modules [3] (Figure 4).

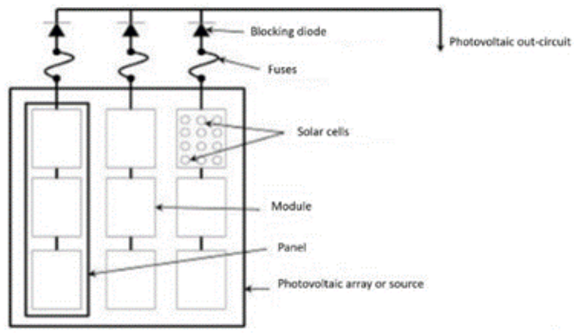


**Figure 4** Component diagram of a string of photovoltaic modules
*Source: NOM-001-SEDE-2012, Capitulo 690*

Photovoltaic modules, on their own, cannot generate consumable electricity for homes or equipment, as the current they emit is not compatible with the conventional power grid. Therefore, it is necessary to connect the modules to a device that transforms the shape of the current signal, and this function is fulfilled by photovoltaic inverters. There are two main types of investors in the market.

The central inverter allows multiple devices to be connected simultaneously, but they are usually large and generate noise (Figure 5). Microinverters, on the other hand, are quieter, more compact, and more versatile, as they are installed close to the modules. However, they have the disadvantage of being more expensive compared to central inverters and do not support so many modules at the same time; newer models generally support no more than four modules at a time (Figure 5).

ISSN 2523-6776

**Figure 5** Example of a central inverter (left) and a micro photovoltaic inverter (right)
*Source: https://www.solarwave.com.mx*

Both modules and inverters are crucial elements in a photovoltaic system. Both are highly susceptible to excessive currents and surges, making it imperative to install protective devices on each component's connections. It is not only a matter of protecting them against overcurrents, but also of preventing current returns from the power grid.

In this sense, to ensure the protection of photovoltaic modules and inverters, specialized devices designed for direct current are used. These act in a similar way to a diode, unlike the protections used for alternating current (Figure 6). This comprehensive approach to protection is essential to safeguard the integrity and optimal performance of components in the PV system. [4].

**Figure 6** Overcurrent protections, on the left, direct current protections, on the right, alternating current protections
*Source: www.chtaixi.com and www.trupper.com*

*Modules in a facility.*

To determine the number of solar panels needed in a photovoltaic system, it is necessary to know the energy consumption of the place in case you want to cover the consumption of a home, company or business.

However, in the case of solar parking lots or photovoltaic plants where there is no precise consumption or target production as such, but rather the aim is to take advantage of the space for the maximum possible energy production, the available area is used to determine the maximum number of panels that can be installed. In addition, the dimensions of the solar panels to be used are also taken into account, as these dimensions vary depending on the maximum power they generate. With these values, equation 1 applies:

$$Generated\ power = \#\ modules * Pmax * HSP * FGF \quad (1)$$

Where "Pmax" is the nominal power of the module under SCT conditions, "HSP" corresponds to the peak solar hours of the region and "FGF" corresponds to the overall operating factor (this value does not have a unit of measurement since it is a quality factor and is usually taken as 0.77).

*Power inverter calculation*

One of the essential components for interconnected photovoltaic systems is the current inverter, this component is responsible for transforming the voltage or waveform from direct current supplied by photovoltaic modules to alternating current so that it can be accepted by the grid [3] . There are currently two types of inverter technology on the market, microinverters and central inverters.

The latter do not specify the maximum number of modules that the central inverter supports, but the maximum voltage and current that they support, so that in order to be able to size the series and parallel lines of the modules (MFV) of a photovoltaic array without damaging the inverter, equations 2 and 3 are used respectively: [ 6 ] so on with the maximum number of microinverters interconnected in the main cable.

*Protections of a photovoltaic system*

The components of a photovoltaic system must be protected against voltage surges, so that the equipment does not break down, as well as protection against electric shocks or lightning rods [ 3 ] ; There are also this type of protections against very high voltages on the market, such as the one in Figure 7.

ISSN 2523-6776

These protections are commonly called ground protection systems and are very important for any electrical system as they protect from permanent damage to the equipment in the event of a current overload or short circuit that could cause a thermal and electrodynamic overload in the equipment or cause severe damage to the personnel who are handling it [7].


**Figure 7** Example of Voltage Protections (SDP)

Along with current protections, voltage protections must be unified in a concentrator box or "String box" whose purpose is, as its name indicates, to concentrate all the multiple connections of an array and provide a means of safe disconnection, these boxes are usually built with fiberglass, resin or aluminum sheets and are widely used in large photovoltaic arrays and generation. An example of these can be seen in Figure 8.

$$Parallel\ MFV = Inverter\ I \max \quad (2)$$

$$MFV\ Isc$$

$$Serial\ MFV = Inverter\ V \max \quad (3)$$
$$MFV\ Vmax$$

**Figure 8** Example of a "String box"

However, with microinverters this problem is reduced to the manufacturer's specifications, since all microinverters on the market must provide the maximum characteristics of the module to be connected (either by its maximum voltage, maximum current, power or number of cells) as well as the maximum number of modules per microinverter and

The current generated by the modules is direct in nature, which means that specially designed DC protection devices are required to protect the equipment. However, in order to protect equipment against current returns, it is essential that the protections work in a coordinated manner, acting as a shut-off valve or diode that prevents the flow of current to the module lines. Many devices, such as circuit breakers, incorporate both functions.

Additionally, to ensure the proper functioning of these devices, the protection must be calculated with a factor of 125% of the maximum current of the equipment, in accordance with NOM-001-SEDE- 2012 [3]. Consequently, when calculating equipment protection, circuit breakers are always determined by equation 4, which includes this factor mentioned above.

$$I\ de\ Proteccion = I \max del\ equipo * 1.25 \quad (4)$$

*Wiring a photovoltaic system*

Modules and inverters are essential in a photovoltaic system and are sensitive to overcurrents and overvoltages. Therefore, the installation of protective devices at the connections of each component is required to prevent damage. In addition to protecting against overcurrents, it is crucial to prevent current returns from the power grid. To achieve this, special protections for direct current are used in the photovoltaic modules, operating in a similar way to a diode, unlike protections for alternating current (Figure 6). This comprehensive protection approach is essential to ensure the integrity and optimal performance of the PV system, for which equation 5 is implemented.

ISSN 2523-6776

| Distance above the roof to the base of the conduit (millimeters) | Temperature adder (°C) |
|---|---|
| From 0 to 13 | 33 |
| More than 13 to 90 | 22 |
| More than 90 to 300 | 17 |
| More than 300 to 900 | 14 |

**Table 1** Ambient temperature adjustments for circular pipes exposed to sunlight, extracted from NOM-001-SEDE-2012, 690 (reconstructed)
*Source: [3]*

Similarly, to determine the temperature factor "Ft" in regions above 30°C ambient temperature, NOM- 001-SEDE-2012 provides table 310-15 (b)(2)(a). This value can be consulted in the table in Figure 9

$$Adjusted\ ampacity = \frac{Required\ ampacity}{Ft * Fc} \quad (5)$$

The "Fc" factor takes into account the number of wires around the conductor, but for joints with less than 5 wires, this value remains constant at "1". As for "Ft", it represents an average ambient temperature value. However, due to temperature variations in cables close to the ground, table 310-15(b)(3)(c) of NOM-001-SEDE-2012 provides additional values that are added to the ambient temperature of the area to determine the actual temperature of the cable. These values are detailed in Table 1 below.

| Para temperaturas ambiente distintas de 30 °C, multiplique las anteriores ampacidades permisibles por el factor correspondiente de los que se indican a continuación: | | | |
|---|---|---|---|
| Temperatura ambiente (°C) | Rango de temperatura del conductor | | |
| | 60 °C | 75 °C | 90 °C |
| 10 o menos | 1.29 | 1.20 | 1.15 |
| 11-15 | 1.22 | 1.15 | 1.12 |
| 16-20 | 1.15 | 1.11 | 1.08 |
| 21-25 | 1.08 | 1.05 | 1.04 |
| 26-30 | 1.00 | 1.00 | 1.00 |
| 31-35 | 0.91 | 0.94 | 0.96 |
| 36-40 | 0.82 | 0.88 | 0.91 |
| 41-45 | 0.71 | 0.82 | 0.87 |
| 46-50 | 0.58 | 0.75 | 0.82 |
| 51-55 | 0.41 | 0.67 | 0.76 |
| 56-60 | - | 0.58 | 0.71 |
| 61-65 | - | 0.47 | 0.65 |
| 66-70 | - | 0.33 | 0.58 |
| 91-75 | - | - | 0.50 |
| 76-80 | - | - | 0.41 |
| 81-85 | - | - | 0.29 |

**Figure 9** Table 310-15(b)(2)(a) Correction Factors based on an ambient temperature of 30 °C, extracted from NOM-001-SEDE-2012,690
*Source: [3]*

It is important to note that not all cables are suitable for all applications. It is necessary to correctly size the wiring according to the different activities. Using the wrong gauge can result in overheating of the wire or unnecessary expense.

To calculate the optimal wire gauge in a photovoltaic system, the maximum ampacity of the wire must be known (using equation 6) and then refer to table 310-15 (b)(16) of NOM- 001-SEDE-2012. This table provides the different types of gauge according to their ampacity. The related information is found in the table shown in Figure 10.

| Tamaño o designación | | Temperatura nominal del conductor [Véase la tabla 310-104(a)] | | | | | |
|---|---|---|---|---|---|---|---|
| | | 60 °C | 75 °C | 90 °C | 60 °C | 75 °C | 90 °C |
| mm2 | AWG o kcmil | TIPOS TW, UF | TIPOS RHW, THHW, THHW-LS, THW, THW-LS, THWN, XHHW, USE, ZW | TIPOS TBS, SA, SIS, FEP, FEPB, MI, RHH, RHW-2, THHN, THHW, THHW-LS, THW-2, THWN-2, USE-2, XHH, XHHW, XHHW-2, ZW-2 | TIPOS UF | TIPOS RHW, XHHW, USE | TIPOS SA, SIS, RHH, RHW-2, USE-2, XHH, XHHW, XHHW-2, ZW-2 |
| | | COBRE | | | ALUMINIO O ALUMINIO RECUBIERTO DE COBRE | | |
| 0.824 | 18** | - | - | 14 | - | - | - |
| 1.31 | 16** | - | - | 18 | - | - | - |
| 2.08 | 14** | 15 | 20 | 25 | - | - | - |
| 3.31 | 12** | 20 | 25 | 30 | - | - | - |
| 5.26 | 10** | 30 | 35 | 40 | - | - | - |
| 8.37 | 8 | 40 | 50 | 55 | - | - | - |
| 13.3 | 6 | 55 | 65 | 75 | 40 | 50 | 55 |
| 21.2 | 4 | 70 | 85 | 95 | 55 | 65 | 75 |
| 26.7 | 3 | 85 | 100 | 115 | 65 | 75 | 85 |
| 33.6 | 2 | 95 | 115 | 130 | 75 | 90 | 100 |
| 42.4 | 1 | 110 | 130 | 145 | 85 | 100 | 115 |
| 53.49 | 1/0 | 125 | 150 | 170 | 100 | 120 | 135 |
| 67.43 | 2/0 | 145 | 175 | 195 | 115 | 135 | 150 |
| 85.01 | 3/0 | 165 | 200 | 225 | 130 | 155 | 175 |
| 107.2 | 4/0 | 195 | 230 | 260 | 150 | 180 | 205 |
| 127 | 250 | 215 | 255 | 290 | 170 | 205 | 230 |
| 152 | 300 | 240 | 285 | 320 | 195 | 230 | 260 |
| 177 | 350 | 260 | 310 | 350 | 210 | 250 | 280 |
| 203 | 400 | 280 | 335 | 380 | 225 | 270 | 305 |
| 253 | 500 | 320 | 380 | 430 | 260 | 310 | 350 |
| 304 | 600 | 350 | 420 | 475 | 285 | 340 | 385 |
| 355 | 700 | 385 | 460 | 520 | 315 | 375 | 425 |
| 380 | 750 | 400 | 475 | 535 | 320 | 385 | 435 |
| 405 | 800 | 410 | 490 | 555 | 330 | 395 | 445 |
| 456 | 900 | 435 | 520 | 585 | 355 | 425 | 480 |

**Figure 10** Table 310-15 (b)(16), Permissible ampacities in insulated conductors, extracted from NOM-001- SEDE-2012, 690
*Source: [3]*

*Calculation of the driver's conduit*

In all photovoltaic installations, the cables are constantly exposed to solar radiation. To protect them from ultraviolet (UV) radiation and high temperatures in the environment, it is necessary to guide the cables through pipes or conduits, especially those that are exposed to weather conditions as established in the Official Mexican Standard [3].

To calculate the appropriate size of the duct, there are tables available, such as Table 5 in Chapter 10 of NOM-001-SEDE-2012 [3] and the Table of "Article 344" of the same regulation. These tables are used by considering the gauge of the cable and the number of conductors to be used, allowing the area of conduit needed to be calculated. Figures 11 and 12 present the relevant data in these tables, respectively.

ISSN 2523-6776

| Tipo | Tamaño | | Diámetro aproximado | Area aproximada |
|---|---|---|---|---|
| | mm2 | AWG o kcmil | mm | mm2 |
| Tipo: FFH-2, RFH-1, RFH-2, RHH*, RHW*, RHW-2*, RHH, RHW, RHW-2, SF-1, SF-2, SFF-1, SFF-2, TF, TFF, THHW, THW, THW-2, TW, XF, XFF | | | | |
| RFH-2, FFH-2 | 0.824 | 18 | 3.454 | 9.355 |
| | 1.31 | 16 | 3.759 | 11.10 |
| RHH, RHW, RHW-2 | 2.08 | 14 | 4.902 | 18.9 |
| | 3.31 | 12 | 5.385 | 22.77 |
| | 5.26 | 10 | 5.994 | 28.19 |
| | 6.63 | 8 | 8.28 | 53.87 |
| | 8.37 | 6 | 9.246 | 67.16 |
| | 21.2 | 4 | 10.46 | 86 |
| | 26.7 | 3 | 11.18 | 98.13 |
| | 33.6 | 2 | 11.99 | 112.9 |
| | 42.4 | 1 | 14.78 | 171.6 |
| | 53.5 | 1/0 | 15.8 | 196.1 |
| | 67.4 | 2/0 | 16.97 | 226.1 |
| | 85.0 | 3/0 | 18.29 | 262.7 |
| | 107 | 4/0 | 19.76 | 306.7 |
| | 127 | 250 | 22.73 | 405.9 |
| | 152 | 300 | 24.13 | 457.3 |
| | 177 | 350 | 25.43 | 507.7 |
| | 203 | 400 | 26.62 | 556.5 |
| | 253 | 500 | 28.78 | 650.5 |
| | 304 | 600 | 31.57 | 782.9 |
| | 355 | 700 | 33.38 | 874.9 |
| | 380 | 750 | 34.24 | 920.8 |
| | 405 | 800 | 35.05 | 965 |
| | 456 | 900 | 36.68 | 1057 |
| | 507 | 1000 | 38.15 | 1143 |
| | 633 | 1250 | 43.92 | 1515 |
| | 760 | 1500 | 47.04 | 1738 |
| | 887 | 1750 | 49.94 | 1959 |
| | 1013 | 2000 | 52.63 | 2175 |

**Figure 11** Table 5, dimensions of conductors according to their caliber, extracted from NOM-001-SEDE-2012, 690-10
*Source: [3]*

| Designación métrica | Tamaño comercial | Diámetro interno | 100% del área total | 60% del área total | Un conductor fr = 53% | Dos conductores fr = 31% | Más de 2 conductores fr = 40% |
|---|---|---|---|---|---|---|---|
| | | mm | mm2 | mm2 | mm2 | mm2 | mm2 |
| 12 | ⅜ | — | — | — | — | — | — |
| 16 | ½ | 16.10 | 204 | 122 | 108 | 63 | 81 |
| 21 | ¾ | 21.20 | 353 | 212 | 187 | 109 | 141 |
| 27 | 1 | 27.00 | 573 | 344 | 303 | 177 | 229 |
| 35 | 1 ¼ | 35.40 | 984 | 591 | 522 | 305 | 394 |
| 41 | 1 ½ | 41.20 | 1333 | 800 | 707 | 413 | 533 |
| 53 | 2 | 52.90 | 2198 | 1319 | 1165 | 681 | 879 |
| 63 | 2 ½ | 63.20 | 3137 | 1882 | 1663 | 972 | 1255 |
| 78 | 3 | 78.50 | 4840 | 2904 | 2565 | 1500 | 1936 |
| 91 | 3 ½ | 90.70 | 6461 | 3877 | 3424 | 2003 | 2584 |
| 103 | 4 | 102.90 | 8316 | 4990 | 4408 | 2578 | 3326 |
| 129 | 5 | 128.90 | 13050 | 7830 | 6916 | 4045 | 5220 |
| 155 | 6 | 154.80 | 18821 | 11292 | 9975 | 5834 | 7528 |

**Figure 12** Table of measurements for heavy metal conduit, extracted from NOM-001-SEDE-2012, Article 344
*Source: [3]*

*Voltage Drop or Voltage*

One of the problems faced by wiring is voltage drop, this is the loss of potential of a conductor caused by the resistance it possesses due to its length [8]. So, in order to calculate the voltage drop by the length of the cable of a system, the following equation 6 is used:

$$e = Z*I*L\ 10*Ef \tag{6}$$

Where "e" is the percentage of the voltage drop, "Z" is the current resistance of the conductors in (this value is obtained from the table in Figure 13), which we can obtain from the NOM-001-SEDE-2012 specifically from table 8 **Ω** [15], "I" is the maximum *km* current flowing through the conductor in Amperes (A), "L" is the length of the cable in meters (m) and "Ef" is the voltage scheme of the system.

| Tamaño (AWG o kcmil) | Area | | Conductores | | | | Resistencia en corriente continua a 75 °C | | |
|---|---|---|---|---|---|---|---|---|---|
| | | | Trenzado | | Total | | Cobre | | Aluminio |
| | | | Cantidad de hilos | Diámetro | Diámetro | Area | No Cubierto | Recubierto | Aluminio |
| | mm2 | kcmil | | mm | mm | mm2 | Ω/km | Ω/km | Ω/km |
| 18 | 0.823 | 1620 | 1 | — | 1.02 | 0.823 | 25.5 | 26.5 | - |
| 18 | 0.823 | 1620 | 7 | 0.39 | 1.16 | 1.06 | 26.1 | 27.7 | - |
| 16 | 1.31 | 2580 | 1 | — | 1.29 | 1.31 | 16 | 16.7 | - |
| 16 | 1.31 | 2580 | 7 | 0.49 | 1.46 | 1.68 | 16.4 | 17.3 | - |
| 14 | 2.08 | 4110 | 1 | — | 1.63 | 2.08 | 10.1 | 10.4 | - |
| 14 | 2.08 | 4110 | 7 | 0.62 | 1.85 | 2.68 | 10.3 | 10.7 | - |
| 12 | 3.31 | 6530 | 1 | — | 2.05 | 3.31 | 6.34 | 6.57 | - |
| 12 | 3.31 | 6530 | 7 | 0.78 | 2.32 | 4.25 | 6.5 | 6.73 | - |
| 10 | 5.261 | 10380 | 1 | — | 2.588 | 5.26 | 3.984 | 4.148 | - |
| 10 | 5.261 | 10380 | 7 | 0.98 | 2.95 | 6.76 | 4.07 | 4.226 | - |
| 8 | 8.367 | 16510 | 1 | — | 3.264 | 8.37 | 2.506 | 2.579 | - |
| 6 | 13.3 | 26240 | 7 | 1.56 | 4.67 | 17.09 | 1.608 | 1.671 | 2.652 |
| 4 | 21.15 | 41740 | 7 | 1.96 | 5.89 | 27.19 | 1.01 | 1.053 | 1.666 |
| 3 | 26.67 | 52620 | 7 | 2.2 | 6.6 | 34.28 | 0.802 | 0.833 | 1.32 |
| 2 | 33.62 | 66360 | 7 | 2.47 | 7.42 | 43.23 | 0.634 | 0.661 | 1.045 |
| 1 | 42.41 | 83690 | 19 | 1.69 | 8.43 | 55.8 | 0.505 | 0.524 | 0.829 |
| 1/0 | 53.49 | 105600 | 19 | 1.89 | 9.45 | 70.41 | 0.399 | 0.415 | 0.66 |
| 2/0 | 67.43 | 133100 | 19 | 2.13 | 10.62 | 88.74 | 0.317 | 0.329 | 0.523 |
| 3/0 | 85.01 | 167800 | 19 | 2.39 | 11.94 | 111.9 | 0.2512 | 0.261 | 0.413 |
| 4/0 | 107.2 | 211600 | 19 | 2.68 | 13.41 | 141.1 | 0.1996 | 0.205 | 0.328 |
| 250 | 127 | — | 37 | 2.09 | 14.61 | 168 | 0.1687 | 0.1753 | 0.2778 |
| 300 | 152 | — | 37 | 2.29 | 16 | 201 | 0.1409 | 0.1463 | 0.2318 |
| 350 | 177 | — | 37 | 2.47 | 17.3 | 235 | 0.1205 | 0.1252 | 0.1984 |
| 400 | 203 | — | 37 | 2.64 | 18.49 | 268 | 0.1053 | 0.1084 | 0.1737 |
| 500 | 253 | — | 37 | 2.95 | 20.65 | 336 | 0.0845 | 0.0869 | 0.1391 |
| 600 | 304 | — | 61 | 2.52 | 22.68 | 404 | 0.0704 | 0.0732 | 0.1159 |

**Figure. 13** Table 8, characteristics of conductors

Partial shading of modules can lead to system efficiency losses or overheating issues due to hot spots. Therefore, in static arrangements it is necessary to calculate the length of the shadows produced by other rows of modules that are in front of them, this is achieved by means of equation 7 [5]:

$$d = L*\sin(\beta)\ \tan(61°-|\boldsymbol{\Phi}|) \tag{7}$$

extracted from NOM-001-SEDE-2012, 690 [3].

*Calculation of Module Shadows*

A photovoltaic module is a grouping of P-N doped silicon cells that harness the photovoltaic effect to produce electricity. It is also made up of other components with the purpose of protecting them from the weather and providing a higher current and voltage than would be obtained with an individual cell, when combined by series and parallel connections [5].

The efficiency of a module can be affected by different factors, such as the position it is in, the temperature, and the amount of sunlight it receives. To determine the optimal position of the module, it is recommended to install it facing the equator (southward in the Northern Hemisphere and northward in the Southern Hemisphere) and with an inclination similar to the latitude of the place where it is located. It is estimated that even with a small difference of ±5 degrees, this could cause a loss of efficiency of at least 1%. [5].

ISSN 2523-6776

One of the main problems that arises when installing modules is the shadow coming from nearby objects or even from other rows of subsequent modules. Although photovoltaic systems are generally intended to be installed in areas that are clear of obstacles that can shade, for systems with several rows of modules, the distance between them can be a determining factor in not generating shade from each other (Figure 14).

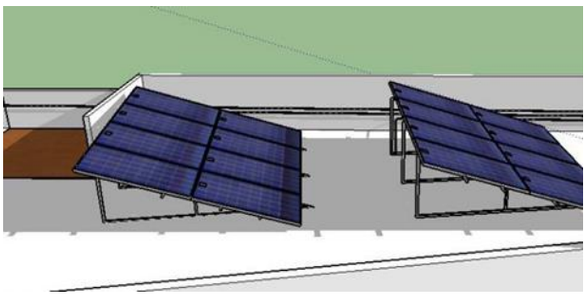

**Figure 14** Example of partial shading between modules
*Source: https://cceea.mx*

Where "d" is the distance of the shadow cast by the module in front, "L" is the length of the module, "β" is the angle of inclination of the module, and "Φ" is the latitude of the place, as shown in Figure 15:

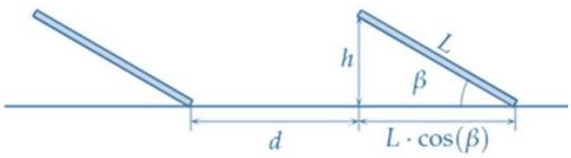


**Figure 15** Exemplification diagram for shading calculation between rows of modules
*Source: [5]*

## Methodology

Below are the calculations developed for the dimensioning of the components of the PV (photovoltaic) system with the information from the tables and figures and with the execution of the equations described in the previous section.

## Module, central inverter and microinverter selection

For the photovoltaic parking, 500W modules of the JASOLAR brand were chosen, the technical sheet of the modules is below in Figure 16 framed in red.

| ELECTRICAL PARAMETERS AT STC | | | | | | |
|---|---|---|---|---|---|---|
| TYPE | JAM66S30 -480/MR | JAM66S30 -485/MR | JAM66S30 -490/MR | JAM66S30 -495/MR | JAM66S30 -500/MR | JAM66S30 -505/MR |
| Rated Maximum Power(Pmax) [W] | 480 | 485 | 490 | 495 | 500 | 505 |
| Open Circuit Voltage(Voc) [V] | 45,07 | 45,20 | 45,33 | 45,46 | 45,59 | 45,72 |
| Maximum Power Voltage(Vmp) [V] | 37,62 | 37,81 | 37,99 | 38,17 | 38,35 | 38,53 |
| Short Circuit Current(Isc) [A] | 13,65 | 13,72 | 13,79 | 13,86 | 13,93 | 14,00 |
| Maximum Power Current(Imp) [A] | 12,76 | 12,83 | 12,90 | 12,97 | 13,04 | 13,11 |
| Module Efficiency [%] | 20,2 | 20,4 | 20,6 | 20,9 | 21,1 | 21,3 |
| Power Tolerance | 0~+5W | | | | | |
| Temperature Coefficient of Isc(α_Isc) | +0,045%/°C | | | | | |
| Temperature Coefficient of Voc(β_Voc) | -0,275%/°C | | | | | |
| Temperature Coefficient of Pmax(γ_Pmp) | -0,350%/°C | | | | | |
| STC | Irradiance 1000W/m², cell temperature 25°C, AM1.5G | | | | | |

**Figure 16** Technical data sheet of the JA SOLAR 500W DEEP BLUE 3.0 model demodule
*Source: https://cdn.autosolar.es/pdf/datasheet-deep-blue-480-505.pdf)*

For the sizing of the parking lot, both proposals from investors were made. Starting with the central inverters, four central inverters were first designated that will share the load of the entire array, given that the modules are 500W and that the array will be divided into four sections of 78 modules so the inverter must be of a power of at least 39kW. The inverter data sheet is below in Figure 17 framed.

Figure.17. Huawei SUN2000-40KTL-M3 central inverter data sheet (Source: https://solar-distribution.bayware.mx/fileadmin/Solar_ Distribution_ MX/04_ Products/03_ Media/Huawei/SUN2000-30-36- 40KTL-M3_MX.pdf)

Knowing then that the nominal power of the inverter is adequate, equations three and four were used to determine the maximum number of modules that are tolerated in parallel and in series. In this way, it is possible to know if the arrangement of the modules is supported by the inverter.

In the case of microinverters, it is only necessary to look for a microinverter that tolerates the largest number of modules while supporting the combined power of the connected modules. In this case, the data sheet of the microinverter used can be found in Figure 19.

ISSN 2523-6776

| DS3D Microinverter Datasheet | |
|---|---|
| Region | LATAM |
| **Input Data (DC)** | |
| Recommended PV Module Power (STC) Range | 315Wp-670Wp+ |
| Peak Power Tracking Voltage | 64V-110V |
| Operating Voltage Range | 52V-120V |
| Maximum Input Voltage | 120V |
| Maximum Input Current | 20A x 2 |
| **Output Data (AC)** | |
| Maximum Continuous Output Power | 2000W |
| Nominal Output Voltage/Range* | 240V/211-264V |
| Adjustable Output Voltage Range | 170V-278V |
| Nominal Output Current | 8.3A |
| Nominal Output Frequency/ Range* | 60Hz/59.3Hz-60.5Hz |
| Adjustable Output Frequency Range | 55Hz-65Hz |
| Output Power Factor | >0.99 |
| Maximum Units per 30A Branch** | 3 |
| **Efficiency** | |
| Peak Efficiency | 97% |
| CEC Efficiency | 96.7% |
| Nominal MPPT Efficiency | 99.5% |
| Night Power Consumption | 20mW |

**Figure 19** Technical data sheet of the Apsystems DS3D model microinverter
*Source:*
*https://drive.google.com/file/d/19I1kDBYEud1W1L5uPc8pU0OfWM14VcAc/view?pli=1*

The data sheet indicates that the maximum number of modules that each microinverter accepts is four, while the maximum number of interconnected microinverters that it accepts is 3. Therefore, to know the number of microinverters needed, it is enough to divide the number of modules of the array (312 modules) by the maximum number of modules per microinverter (4) giving a total of 78 microinverters, however, since the microinverter resists up to three of these interconnected, to know the main lines of the entire array it is enough to make a simple division:

$\#\ total\ MFV$

$Serial\ MFV$ = 1,100 $V$ = 28.68 ~ 28 $modelos$

$Total\ strings = MFV\ per\ inverter * Max\ conected\ inverters$ 312 38.35 $V$ 40 $A$

$Parallel\ MFV$ =13.03 = 3.07 ~ 3 $modules$

$Total\ inverter$ == 26 $strings$
$4 * 3$

These 26 branches will be the ones that carry the energy of the entire system, Figure 20 shows a connection diagram of this option.

With the results obtained, it can be concluded that each section should be of no less than three strings in parallel of 28 modules each. So dividing the space of proposal b into four sections yields a connection diagram like the example below (Figure 18).

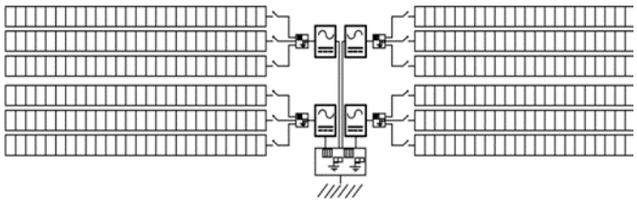

**Figure 18** Diagram of connection of the components of the array with central inverters

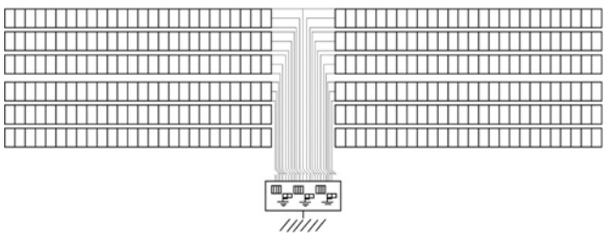

**Figure 20** Diagram of connections of the components of the array with microinverters

*Calculation of protections*

For the system with central inverters, the main protections must first be identified, a direct current protection for the modules at the end of each string of each annex, a direct current protection for the total set of modules in parallel of each annex along with a voltage protection and finally, an alternating current protection for all central inverters together as well as a voltage protection. To better understand this list, Figure 21 shows a diagram with the connection of the protections.

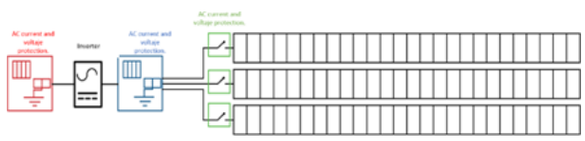

**Figure 21** Central inverter protection diagram

To calculate the protection of each string, the indication of the NOM-001-SEDE-2012 is followed, which indicates that for the protection equipment, the maximum current of the equipment must be dimensioned by the protection factor of 125%, so that to know the current of the protective equipment that is planned to be used, this factor must be multiplied by the short-circuit current of the module (this value can be consulted in the data sheet of the Figure 19)

$I\ de\ proteccion = Isc\ del\ modulo * 1.25$

$I\ de\ proteccion$ = 13.93 $A * 1.25$ = 17.41 $A$

ISSN 2523-6776

The same NOM-001-SEDE-2012 specifically in chapter 2, Article 240, Section 6 where the different values that we find for 50 safety switches are indicated, being the list (in amperes)15, 16, 20, 25, 30, 32, 35, 40, 45, 50, 60, 63, 70, 80, 90, 100, 110,125, etc. Therefore, all current switches and protections will be jumped to the immediately higher value as the case may be, that is, for this case, 20 A switches were contemplated and as the diagram marks these must be for direct current. For the second protection (blue color) the same protections are used as in the previous case, because the current remains the same, and in the same way one is installed for each string of modules.

For the third protection (red), the same pattern was followed with the difference that now instead of using the short-circuit current of the module, the maximum input current obtained from the sheet in Figure 21 was used. In addition, since the protection


**Figure 22** On the left, DC protection switch (20 A), on the right, AC protection switch (50 A)

For the option with microinverters, the protection of the components is reduced and simpler, because the microinverter is installed so close to the modules, it does not need protection for each module. Only one protection for each main branch of the array (26 branches), and to select a circuit breaker the same procedure dictated by NOM-001-SEDE-2012 is used and the maximum output current of the inverter (obtained from Figure 24) is multiplied by the number of microinverters per branch at 125%:

$$I\ de\ proteccion = Imax\ out * inverters\ per\ string * 1.25$$

$$Proteccion\ current = 24\ A * 3 * 1.25 = 90\ A$$

*Wiring calculation*

For the system with central inverters it was taken into account that the cables of the array will go as close as possible to the ground, in table 1 we obtain that the temperature factor is 33°C, this factor is added to the average ambient temperature of the area, which is 22.1°C, giving a total temperature of 55.1°C. Using this value, table 6.1 was consulted to obtain the temperature factor of the conductor in a range of 75°C, which is 0.67. Since the factor Fc is replaced by "1" and the current is the maximum output of the inverter (Table 3) multiplied by the number of central inverters, applying equation 5 is the following: 63.8 $A * 4$ is inverter, direct current protections are no longer contemplated but alternating current protections and

$$Adjusted\ ampacity\ required = 0.67 * 1 = 380\ A$$

The corresponding procedure was carried out. Figure 22 below shows examples of switches that can be installed in the array (these protections will go inside a concentrator box with a general disconnect switch):

$$I\ de\ proteccion = Isc\ del\ inversor * 1.25$$

$$I\ de\ proteccion = 40\ A * 1.25 = 50\ A$$

Since it is a three-phase system, i.e. with three current-carrying lines, this ampacity is divided into three, giving a total of 127 A each. With this ampacity, the table in Figure 12 was consulted to find the gauge of the cable, being a 2/0 gauge, with a designation AWG of copper at a temperature range of 75°C.

For the calculation of the voltage drop, using the value of the 2/0 gauge corresponding to this dimensioning, it was obtained that the resistance offered by the cable was 0.261 Ω/km from the table in Figure 13. Finally, a cable distance of 65 meters was figured out and equation 6 was applied:

$$0.261\ \Omega * 190\ A * 65\ mts$$

$$Tension\ fall = \frac{}{km} = 0.73\% < 3\%\ 10 * 440v$$

ISSN 2523-6776

As can be seen from the above result, the voltage drop does not exceed the limit established by the NOM of 3%, so the corresponding calculations and values obtained are acceptable.

Finally, for the option with microinverters, as with the central inverters section, table 1 indicated together with the average ambient temperature of the place that the temperature adder value is 55.1°C. Consulting the temperature value with the table in Figure 12, the temperature factor of the conductor was extracted in a range of 75°C, which was 0.67. Equation 6 was implemented to determine the adjusted required ampacity using the output current of each branch as the inverter current value, multiplied by the number of microinverters:

column of "two or more conductors" for the exact cross-sectional area for the conduit, it was determined that the 35-gauge conduit () is the most suitable. 4

Finally, for the proposal with microinverters: each cable is 800 gauge, when consulted in the table in Figure 15 a total area result of 405 mm2 is obtained for each 800 gauge cable. Because it is a two-phase system (three wires), due to the maximum voltage output of the inverter (240V), the total wiring area is 1215mm$^2$. From the table in Figure 16 it is concluded that a 53 gauge (2") conduit is needed.

*Module distribution and shading calculation*

For the dimensioning of the parking lot of the technological institute of the lagoon, a space was considered behind the postgraduate study area with dimensions of 18 meters wide by 53 meters long with a latitude of 25° (Figure 23). And 500W modules of the JA SOLAR brand were contemplated, measuring approximately one meter wide by two meters long.

$Adjusted\ ampacity\ required$ = 24.9 $A$ ∗ 26 0.67 ∗ 1 = 966 $A$

As in the previous case, the load must be divided into two cable lines (because microinverters have a two- phase voltage output). In this way, each line of cable will have an amperage of 483 A. Thus, using the table in Figure 13 it is obtained that each of the cables must be of 800 gauge.

With the gauge of the cable and using the table in Figure 14, the resistance of theconductor was obtained, which is 0.0544, and the $\Omega\ km$ voltage drop of the cables was calculated, using the ampacity calculated previously and the distance of the cable speculated, applying equation 6 as follows:

0.0544 $\Omega$ ∗ 483 $A$ ∗ 65 $mts$

$Tension\ fall$ = $k$m = 0.77% < 3% 10 ∗ 220$v$

The voltage drop does not exceed the established limit of 3%, therefore, it does not present significant losses.

*Conduit calculation*

Table 5 located in chapter 10 of the NOM (Figure 15) was used to calculate the Conduit of the option with central inverters, where the diameters in millimeters of each wire gauge are shown, and the 3/0 gauge belonging to the array was located, resulting in an area of 98.13 mm2 for each wire. Since it is a three- phase system (four wires) the total area is 392.52 mm2. By looking at the table in Figure 16, in the


**Figure 23** Photograph of the parking lot area
*Source: Google Maps*

For this space, three options were contemplated for the arrangement of the modules and their 3D models were made using the Sketchup tool, option a: contemplates a single plate of modules that covers the entire extension of the parking area (Figure 24). Option b divides the parking area into two three-module-tall sections at the edge of the parking lot (Figure 25). Finally, option c divides the parking area into three sections of two modules high each (Figure 26) taking into account a standard PV module measurement of one meter wide by two meters long.

ISSN 2523-6776

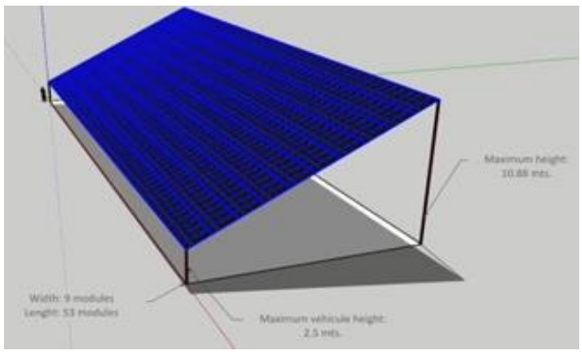


**Figure 24** Proposal "a"

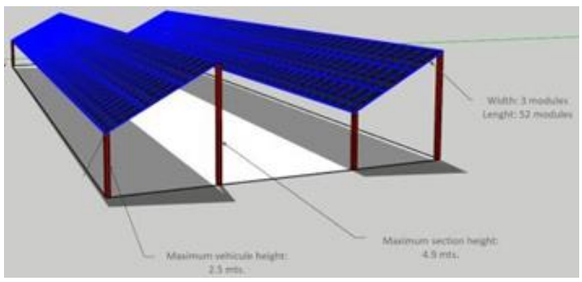


**Figure 25** Proposal "b"

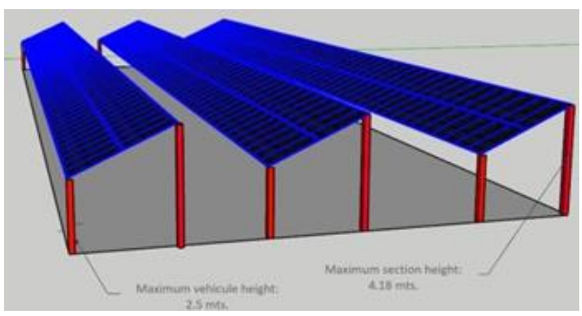


**Figure 26** Proposal "c"

Analyzing the advantages and disadvantages of each arrangement, it was decided to use option b since it is the one that best adapts to the predetermined way of parking cars and is the one that best preserves the distances between cars, having a total of 312 modules distributed in two sections of three modules wide by 52 modules long. Thus, the distance between the two corresponding rows was calculated based on the diagram in Figure 27.

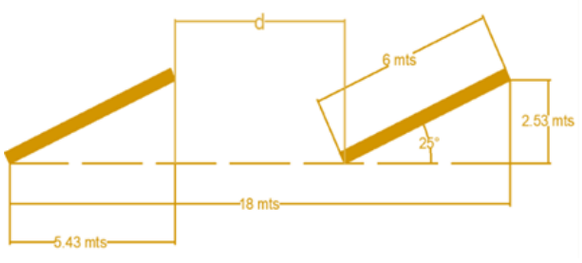


**Figure 27** Distance diagram of proposal b

When applying equation 7 taking into account a modulus of 1 meter wide by two meters long, the distance of the longest shadow is as follows:

Table 2 below shows the estimated costs for the photovoltaic array with central inverters. Table 3 shows the estimated cost of the components of the photovoltaic array with microinverters; The costs of both tables were reflected taking into account the prices that manufacturers advertise on their platforms, as well as the shipping costs of some of these.

| system element | units | unit prices (MNX) | total price |
|---|---|---|---|
| Modulo JASOLAR 500W | 312 | 4,700.00 | 1,466,400.00 |
| Inversor central Huaweii | 4 | 33,200.00 | 132,800.00 |
| Noark 20A thermomagnetic switch | 12 | 186.61 | 2,239.32 |
| Concentrator Boxes (Modules & Inverters) | 5 | 500.00 | 2,500.00 |
| Chtaixi 20A Protection Switch | 24 | 238.00 | 5,712.00 |
| Volfgang SDP Overvoltage Protections | 10 | 245.00 | 2,450.00 |
| High Voltage Disconnect Switches | 5 | 405.00 | 2,025.00 |
| AWG calibre 3/0 (mts) | 195 | 229.00 | 44,655.00 |
| Cable AWG calibre 10 (mts) | 104 | 380.00 | 39,520.00 |
| 1 1/4 (MTS) Conduit | 65 | 335.00 | 21,775.00 |
| Total price | | | 1,720,076.32 |

**Table 2** Costs for sizing with central inverters.

$$d = L * \sin(\beta) \tan(61° - |\Phi|$$

From the table above we can see that 85% of the installation costs would be only for the purchase of the modules since it is one of the most expensive

$$d = 6mts * \sin(25°) \tan(67° - |25.53°|) = 2.86\ m$$

components along with the central inverters and their overwhelming quantity. The cable also results in a significant expense, making up approximately 5% of being that the shade reaches a maximum length of 2.86 meters, that the horizontal distance of each section is 5.43 meters and that the width of the parking space is 18 meters, that leaves a margin of distances of between 2.86 meters to 4.28 meters of distance, enough space to perform displacement maneuvers for the accommodation of vehicles and it is verified that the shadows do not interpose each other.

ISSN 2523-6776

## Results

the total dimensioning. Costs could be reduced by installing a substation close to the facility. Without taking into account the labor and structures of the modules, the total cost of the arrangement could amount to approximately two million Mexican pesos.

| SYSTEM ELEMENT | UNITS | UNIT PRICE S (MNX) | TOTAL PRICE |
|---|---|---|---|
| Modulo JASOLAR 500W | 312 | 4,700.00 | 1,466,400.00 |
| DS3D Micro Inverter | 78 | 9,799.00 | 764,322.00 |
| Concentrator Boxes (Modules & Inverters) | 1 | 500.00 | 500.00 |
| Chtaixi 20A Protection Switch | 24 | 238.00 | 5,712.00 |
| LT1-40 Overvoltage Protections | 2 | 245.00 | 490.00 |
| High Voltage Disconnect Switches | 1 | 405.00 | 405.00 |
| Cable AWG calibre 800 (mts) | 195 | 309.00 | 60,255.00 |
| Cable AWG calibre 10 (mts) | 104 | 380.00 | 39,520.00 |
| 2" Conduit (mts) | 40 | 275.00 | 11,000.00 |
| Total price | | | 2,348,604.00 |

**Table 3** Costs for sizing with microinverters

As can be seen in the tables, the cost of sizing using central inverters can be up to 27% cheaper, that is, around 628 thousand pesos cheaper than with the installation of microinverters.

This is due to the fact that there are multiple inverter parts installed, which in the middle of 2023 are not entirely cheap compared to other technologies such as central inverters. One of the main advantages of using microinverters is the fact that the number of concentrator boxes is reduced and that the wiring system is more compact overall. However, due to the very nature of microinverters, they increase the costs of the cable to be used, as well as its quantity and also that of the conduit. Figure 30 shows in detail the final arrangement of the complete array performed in Sketchup.

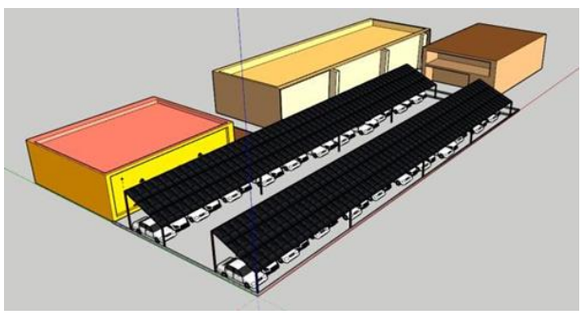

**Figure 28** Aerial view in perspective 3/4 of the arrangement

As can be seen in the Figure, the number of vehicles is very close to the number shown in Figure 17, and thanks to the software it was verified that there is no shading factor that alters the efficiency of the parking.

## Conclusions

In this chapter, a hypothetical analysis was carried out with the aim of sizing a photovoltaic system that could cover the needs of parking in the area of postgraduate studies of the Technological Institute of La Laguna. An exhaustive list of various inverter and module configurations was made, evaluating their respective advantages and disadvantages. A solution using central inverters was proposed, as well as another using microinverters, also considering the associated costs.

After careful analysis, it was concluded that choosing central inverters instead of microinverters for current conversion could reduce production costs by 27%. In addition, this option would allow a three-phase connection, simplifying the sizing of the conductive medium and achieving a more efficient connection between the modules.

The dimensioned photovoltaic system has a generation capacity of 750 kW per day, with an approximate cost of two million Mexican pesos. To support this choice, the surrounding buildings' electricity consumption was estimated at 739 kW per day, indicating that the proposed sizing would be able to fully meet the energy needs of the graduate area.

## Acknowledgments

CONAHCYT for grants, TecNM projects and PRODE.

## References

1. Solar, E. (2007). Photovoltaic solar energy. Available in: http://www.enginyeria-classea.cat/pdf-formativos/Cuaderno_FOTOVOLTAICA.pdf

2. Cieza Coronado, J. C. (2018). Dimensioning of a photovoltaic system for the electrical lighting installations in the lancelot hostel located in Chiclayo-Chiclayo-Lambayeque.

3. L. Aurora and O. Salgado, "NORMA Oficial Mexicana NOM-001-SEDE-2012, Instalaciones Eléctricas (utilización)". [Online]. Available in: www.dof.gob.mx/normasOficiales/4951/ SENER/SE NER.html

4. Gilberto Enríquez Harper, "Practical Guide for the Calculation of eléctricas_ Installations Based on Technical Standards for Electrical Installations (PDFDrive)".

5. O. P. Lamigueiro, "Photovoltaic Solar Energy". 2015. [Online]. Available in: https://github.com/oscarperpinan/esf

6. H. López, "Design of a photovoltaic system integrated into the grid for the parking area of the technological university of Salamanca", October 2014.

7. Cieza Coronado, J. C. (2018). Dimensioning of a photovoltaic system for the electrical lighting installations in the lancelot hostel located in Chiclayo-Chiclayo-Lambayeque.

8. Cieza Coronado, J. C. (2018). Dimensioning of a photovoltaic system for the electrical lighting installations in the lancelot hostel located in Chiclayo-Chiclayo-Lambayeque.

ISSN 2523-6776

# [Title in Times New Roman and Bold No. 14 in English and Spanish]

Surname (IN UPPERCASE), Name 1st Author†*, Surname (IN UPPERCASE), Name 1st Co-author, Surname (IN UPPERCASE), Name 2nd Co-author and Surname (IN UPPERCASE), Name 3rd Co-author

*Institutional Affiliation of Author including Dependency (No.10 Times New Roman and Italic)*

*International Identification of Science - Technology and Innovation*

ID 1st Author: (ORC ID - Researcher ID Thomson, arXiv Author ID - PubMed Author ID - Open ID) and CVU 1st author: (Scholar-PNPC or SNI-CONACYT) (No.10 Times New Roman)

ID 1st Co-author: (ORC ID - Researcher ID Thomson, arXiv Author ID - PubMed Author ID - Open ID) and CVU 1st co-author: (Scholar or SNI) (No.10 Times New Roman)

ID 2nd Co-author: (ORC ID - Researcher ID Thomson, arXiv Author ID - PubMed Author ID - Open ID) and CVU 2nd co-author: (Scholar or SNI) (No.10 Times New Roman)

ID 3rd Co-author: (ORC ID - Researcher ID Thomson, arXiv Author ID - PubMed Author ID - Open ID) and CVU 3rd co-author: (Scholar or SNI) (No.10 Times New Roman)

(Report Submission Date: Month, Day, and Year); Accepted (Insert date of Acceptance: Use Only ECORFAN)

**Abstract (In English, 150-200 words)**

Objectives
Methodology
Contribution

**Abstract (In Spanish, 150-200 words)**

Objectives
Methodology
Contribution

**Keywords (In English)**

Indicate 3 keywords in Times New Roman and Bold No. 10

**Keywords (In Spanish)**

Indicate 3 keywords in Times New Roman and Bold No. 10

**Citation:** Surname (IN UPPERCASE), Name 1st Author, Surname (IN UPPERCASE), Name 1st Co-author, Surname (IN UPPERCASE), Name 2nd Co-author and Surname (IN UPPERCASE), Name 3rd Co-author. Paper Title. Journal of Technological Engineering. Year 1-1: 1-11 [Times New Roman No.10]

* Correspondence to Author (example@example.org)
† Researcher contributing as first author.

## Introduction

Text in Times New Roman No.12, single space.

General explanation of the subject and explain why it is important.

What is your added value with respect to other techniques?

Clearly focus each of its features

Clearly explain the problem to be solved and the central hypothesis.

Explanation of sections Article.

## Development of headings and subheadings of the article with subsequent numbers

[Title No.12 in Times New Roman, single spaced and bold]

Products in development No.12 Times New Roman, single spaced.

## Including graphs, figures and tables-Editable

In the article content any graphic, table and figure should be editable formats that can change size, type and number of letter, for the purposes of edition, these must be high quality, not pixelated and should be noticeable even reducing image scale.

[Indicating the title at the bottom with No.10 and Times New Roman Bold]

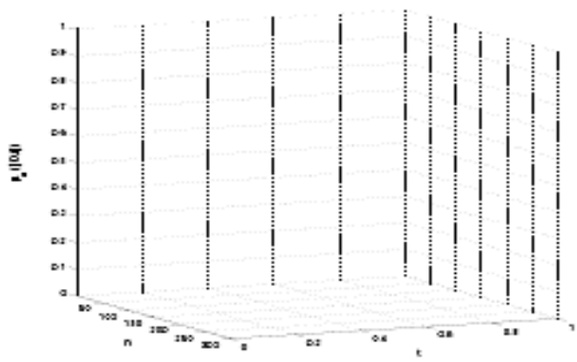

**Graphic 1** Title and *Source (in italics)*

Should not be images-everything must be editable.

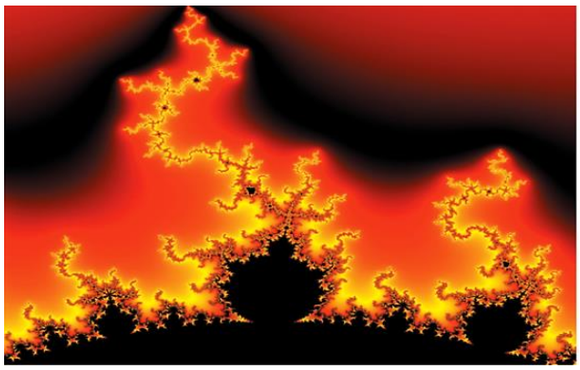

**Figure 1** Title and *Source (in italics)*

Should not be images-everything must be editable.

| | | | | |
|---|---|---|---|---|
| | | | | |
| | | | | |
| | | | | |
| | | | | |

**Table 1** Title and *Source (in italics)*

Should not be images-everything must be editable.

Each article shall present separately in **3 folders**: a) Figures, b) Charts and c) Tables in .JPG format, indicating the number and sequential Bold Title.

**For the use of equations, noted as follows:**

$$Y_{ij} = \alpha + \sum_{h=1}^{r} \beta_h X_{hij} + u_j + e_{ij} \quad (1)$$

Must be editable and number aligned on the right side.

## Methodology

Develop give the meaning of the variables in linear writing and important is the comparison of the used criteria.

## Results

The results shall be by section of the article.

## Annexes

Tables and adequate sources

## Thanks

Indicate if they were financed by any institution, University or company.

ISSN 2523-6776

**Conclusions**

Explain clearly the results and possibilities of improvement.

**References**

Use APA system. Should not be numbered, nor with bullets, however if necessary numbering will be because reference or mention is made somewhere in the Article.

Use Roman Alphabet, all references you have used must be in the Roman Alphabet, even if you have quoted an Article, book in any of the official languages of the United Nations (English, French, German, Chinese, Russian, Portuguese, Italian, Spanish, Arabic), you must write the reference in Roman script and not in any of the official languages.

**Technical Specifications**

Each article must submit your dates into a Word document (.docx):

Journal Name
Article title
Abstract
Keywords
Article sections, for example:

*1. Introduction*
*2. Description of the method*
*3. Analysis from the regression demand curve*
*4. Results*
*5. Thanks*
*6. Conclusions*
*7. References*

Author Name (s)
Email Correspondence to Author
References

**Intellectual Property Requirements for editing:**

- Authentic Signature in Color of Originality Format Author and Co-authors.
- Authentic Signature in Color of the Acceptance Format of Author and Co-authors.
- Authentic Signature in Color of the Conflict of Interest Format of Author and Co-authors.

ISSN 2523-6776

**Reservation to Editorial Policy**

Journal of Technological Engineering reserves the right to make editorial changes required to adapt the Articles to the Editorial Policy of the Journal. Once the Article is accepted in its final version, the Journal will send the author the proofs for review. ECORFAN® will only accept the correction of errata and errors or omissions arising from the editing process of the Journal, reserving in full the copyrights and content dissemination. No deletions, substitutions or additions that alter the formation of the Article will be accepted.

**Code of Ethics - Good Practices and Declaration of Solution to Editorial Conflicts**

**Declaration of Originality and unpublished character of the Article, of Authors, on the obtaining of data and interpretation of results, Acknowledgments, Conflict of interests, Assignment of rights and Distribution**

The ECORFAN-Mexico, S.C. Management claims to Authors of Articles that its content must be original, unpublished and of Scientific, Technological and Innovation content to be submitted for evaluation.

The Authors signing the Article must be the same that have contributed to its conception, realization and development, as well as obtaining the data, interpreting the results, drafting and reviewing it. The Corresponding Author of the proposed Article will request the form that follows.

Article title:

– The sending of an Article to Journal of Technological Engineering emanates the commitment of the author not to submit it simultaneously to the consideration of other series publications for it must complement the Format of Originality for its Article, unless it is rejected by the Arbitration Committee, it may be withdrawn.

– None of the data presented in this article has been plagiarized or invented. The original data are clearly distinguished from those already published. And it is known of the test in PLAGSCAN if a level of plagiarism is detected Positive will not proceed to arbitrate.

– References are cited on which the information contained in the Article is based, as well as theories and data from other previously published Articles.

– The authors sign the Format of Authorization for their Article to be disseminated by means that ECORFAN-Mexico, S.C. In its Holding Taiwan considers pertinent for disclosure and diffusion of its Article its Rights of Work.

– Consent has been obtained from those who have contributed unpublished data obtained through verbal or written communication, and such communication and Authorship are adequately identified.

– The Author and Co-Authors who sign this work have participated in its planning, design and execution, as well as in the interpretation of the results. They also critically reviewed the paper, approved its final version and agreed with its publication.

– No signature responsible for the work has been omitted and the criteria of Scientific Authorization are satisfied.

– The results of this Article have been interpreted objectively. Any results contrary to the point of view of those who sign are exposed and discussed in the Article.

## Copyright and Access

The publication of this Article supposes the transfer of the copyright to ECORFAN-Mexico, SC in its Holding Taiwan for its Journal of Technological Engineering, which reserves the right to distribute on the Web the published version of the Article and the making available of the Article in This format supposes for its Authors the fulfilment of what is established in the Law of Science and Technology of the United Mexican States, regarding the obligation to allow access to the results of Scientific Research.

Article Title:

| Name and Surnames of the Contact Author and the Co-authors | Signature |
|---|---|
| 1. | |
| 2. | |
| 3. | |
| 4. | |

## Principles of Ethics and Declaration of Solution to Editorial Conflicts

### Editor Responsibilities

The Publisher undertakes to guarantee the confidentiality of the evaluation process, it may not disclose to the Arbitrators the identity of the Authors, nor may it reveal the identity of the Arbitrators at any time.

The Editor assumes the responsibility to properly inform the Author of the stage of the editorial process in which the text is sent, as well as the resolutions of Double-Blind Review.

The Editor should evaluate manuscripts and their intellectual content without distinction of race, gender, sexual orientation, religious beliefs, ethnicity, nationality, or the political philosophy of the Authors.

The Editor and his editing team of ECORFAN® Holdings will not disclose any information about Articles submitted to anyone other than the corresponding Author.

The Editor should make fair and impartial decisions and ensure a fair Double-Blind Review.

### Responsibilities of the Editorial Board

The description of the peer review processes is made known by the Editorial Board in order that the Authors know what the evaluation criteria are and will always be willing to justify any controversy in the evaluation process. In case of Plagiarism Detection to the Article the Committee notifies the Authors for Violation to the Right of Scientific, Technological and Innovation Authorization.

### Responsibilities of the Arbitration Committee

The Arbitrators undertake to notify about any unethical conduct by the Authors and to indicate all the information that may be reason to reject the publication of the Articles. In addition, they must undertake to keep confidential information related to the Articles they evaluate.

Any manuscript received for your arbitration must be treated as confidential, should not be displayed or discussed with other experts, except with the permission of the Editor.

The Arbitrators must be conducted objectively, any personal criticism of the Author is inappropriate.

The Arbitrators must express their points of view with clarity and with valid arguments that contribute to the Scientific, Technological and Innovation of the Author.

The Arbitrators should not evaluate manuscripts in which they have conflicts of interest and have been notified to the Editor before submitting the Article for Double-Blind Review.

**Responsibilities of the Authors**

Authors must guarantee that their articles are the product of their original work and that the data has been obtained ethically.

Authors must ensure that they have not been previously published or that they are not considered in another serial publication.

Authors must strictly follow the rules for the publication of Defined Articles by the Editorial Board.

The authors have requested that the text in all its forms be an unethical editorial behavior and is unacceptable, consequently, any manuscript that incurs in plagiarism is eliminated and not considered for publication.

Authors should cite publications that have been influential in the nature of the Article submitted to arbitration.

**Information services**

**Indexation - Bases and Repositories**

RESEARCH GATE (Germany)
GOOGLE SCHOLAR (Citation indices-Google)
MENDELEY (Bibliographic References Manager)
REDIB (Ibero-American Network of Innovation and Scientific Knowledge- CSIC)
HISPANA (Information and Bibliographic Orientation-Spain)

**Publishing Services**

Citation and Index Identification H
Management of Originality Format and Authorization
Testing Article with PLAGSCAN
Article Evaluation
Certificate of Double-Blind Review
Article Edition
Web layout
Indexing and Repository
ArticleTranslation
Article Publication
Certificate of Article
Service Billing

**Editorial Policy and Management**

69 Street. YongHe district, ZhongXin. Taipei-Taiwan. Phones: +52 1 55 6159 2296, +52 1 55 1260 0355, +52 1 55 6034 9181; Email: contact@ecorfan.org www.ecorfan.org

# Journal of Technological Engineering




2523 6776
ISSN 2523 - 6776
www.ecorfan.org